Earth’s background free oscillations

Kiwamu Nishida,
Earthquake Research Institute,
University of Tokyo

Background wavefield

Persistent excitation by distributed sources

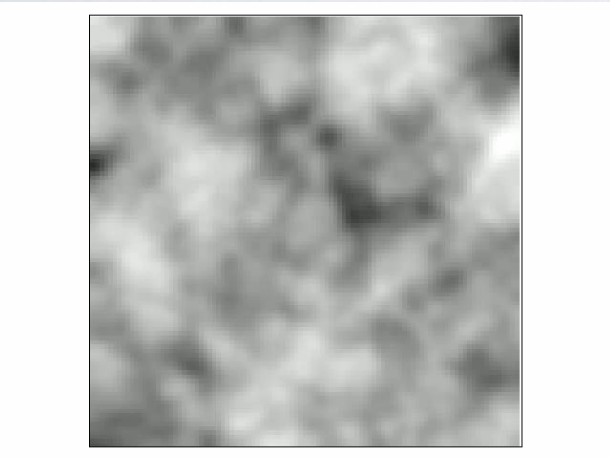

Transient by an event

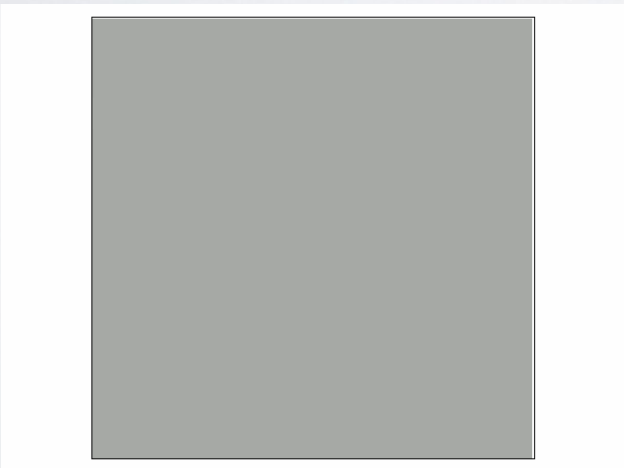

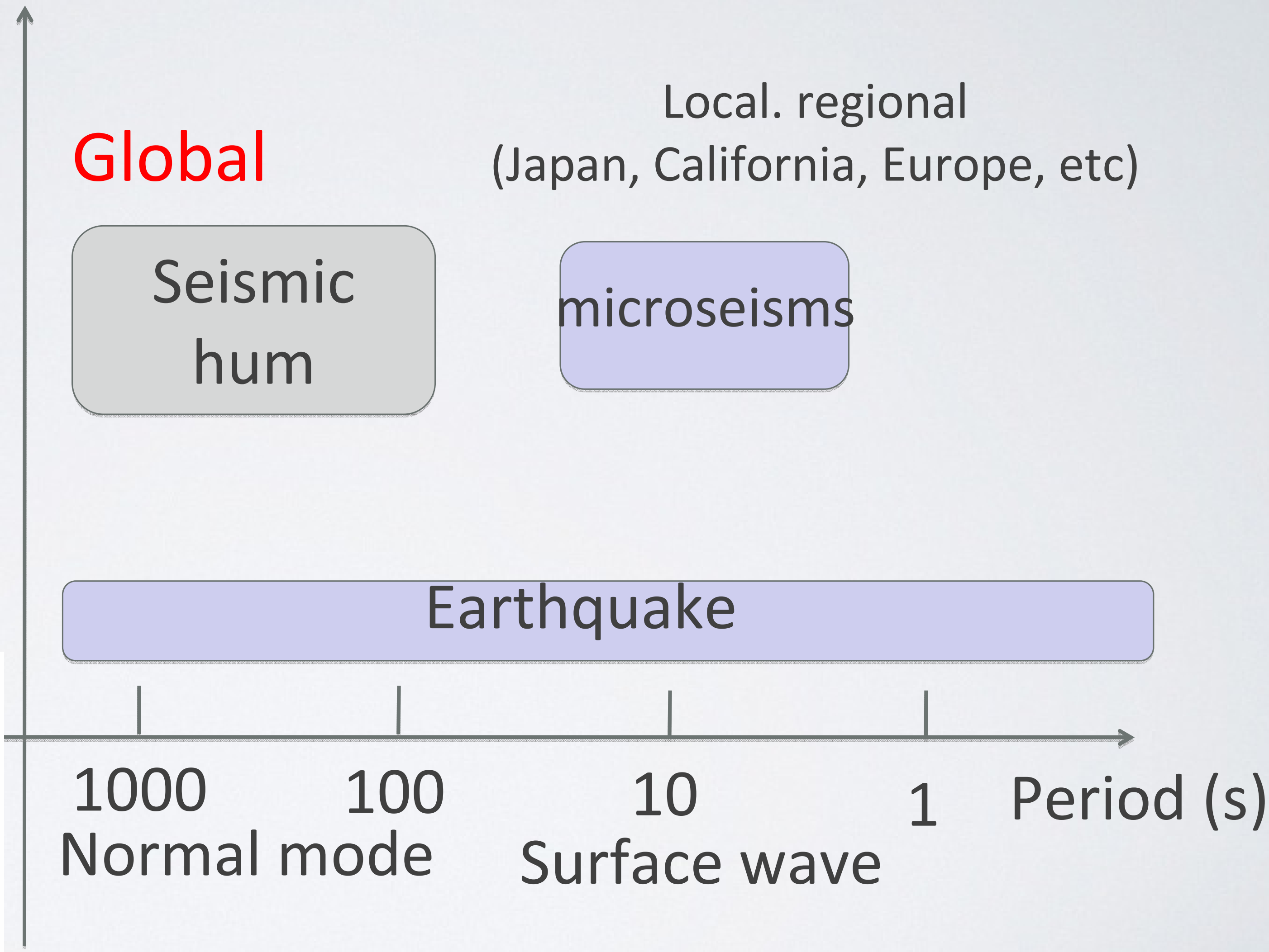

Global body wave propagation

Discovery of Earth's background free oscillations (seismic hum) [1998]

- Persistent excitation of fundamental spheroidal modes from 2 to 20 mHz
- Annual variations of their amplitudes
- Acoustic resonance: atmospheric turbulence

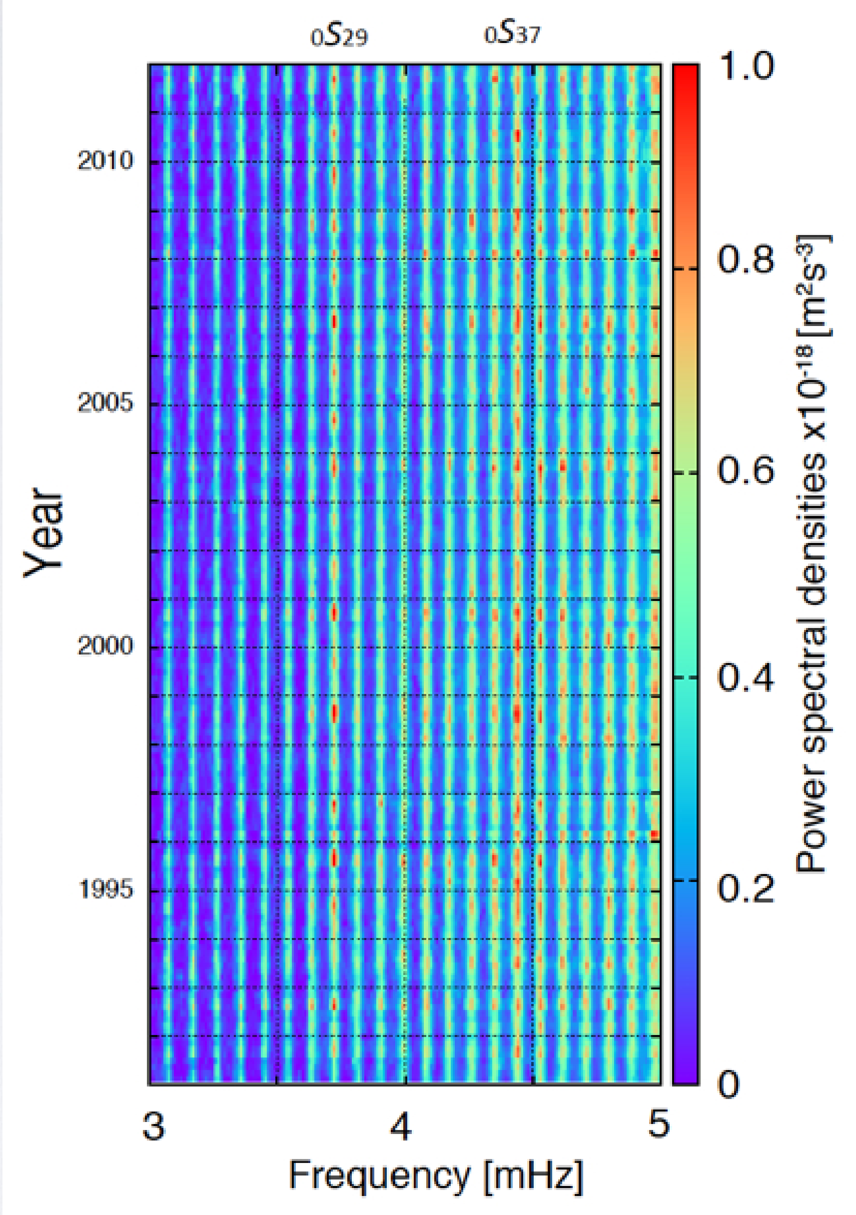

Nishida [2012]

Source distribution

- Strong excitation: Oceanic infragravity waves
  - In the north Pacific in winter
  - In the southern hemisphere in summer

（1） Array observation

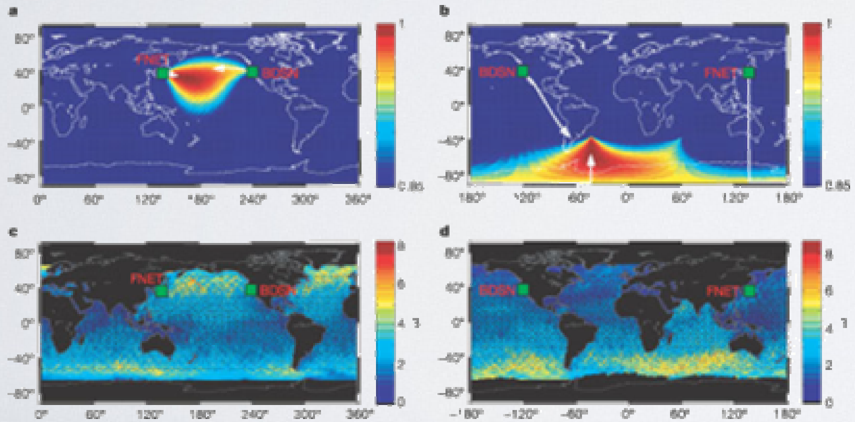

Rhie and Romonowicz [2004]

（2） Modeling of cross spectra

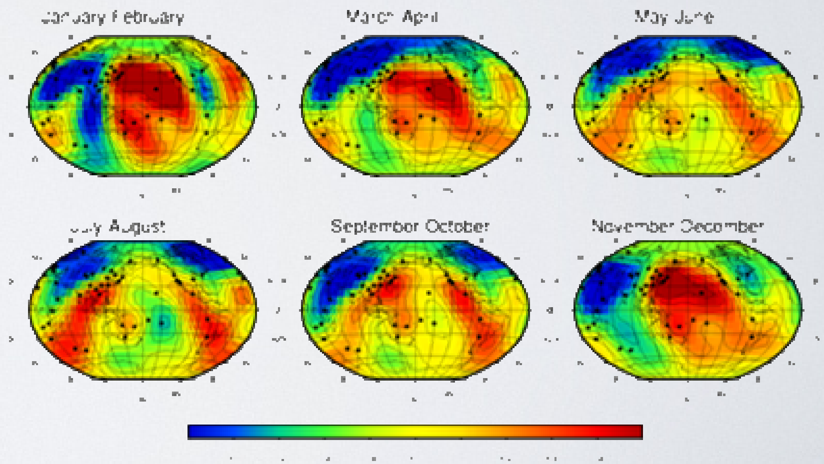

Nishida and Fukao [2007]

Pressure sources are dominant.

Discovery of horizontal hum

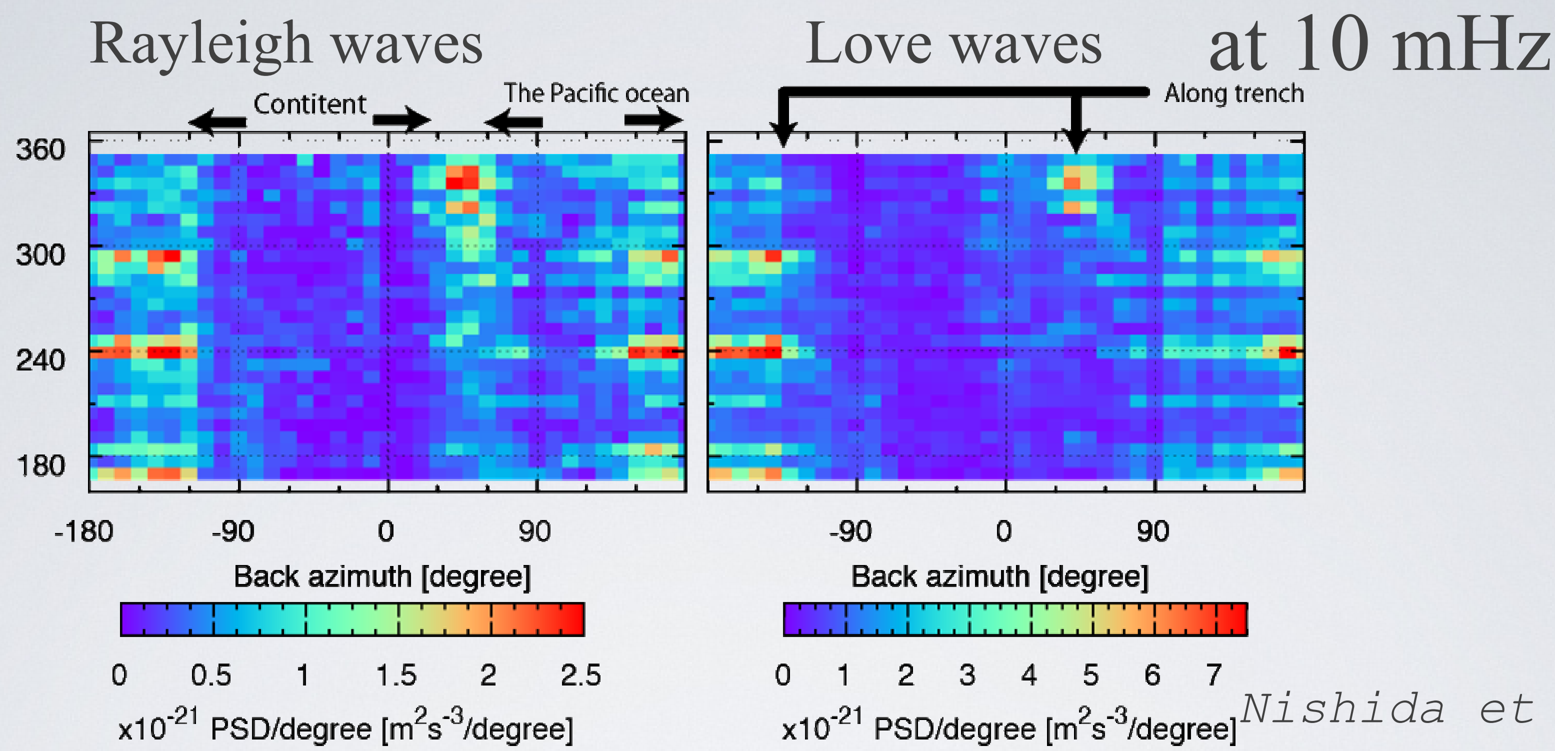

Nishida et al. (2008)

Love wave amplitudes ~ 3xRayleigh wave amplitudes (10-100 mHz)

Similar azimuthal patterns

Background Love waves from 3 to 5 mHz *Kurrle and Widmer (2008)*

Random shear traction on the seafloor

Origins of seismic hum

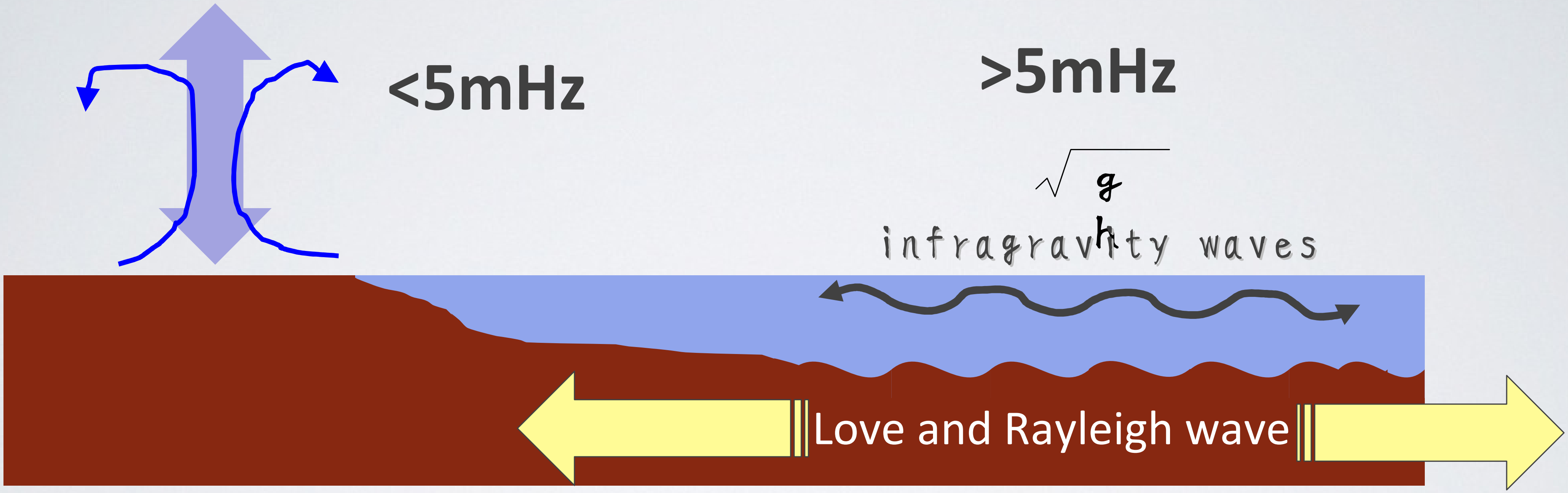

Abyssal plane: Linear topographic coupling
[Fukao et al, 2010; Saito, 2010]

Inference of the force system

Cross-correlation analysis: Data set

Cross spectra

$$\begin{pmatrix} \Phi^d_{\theta\theta} \\ \Phi^d_{\phi\phi} \\ \Phi^d_{zz} \end{pmatrix}$$

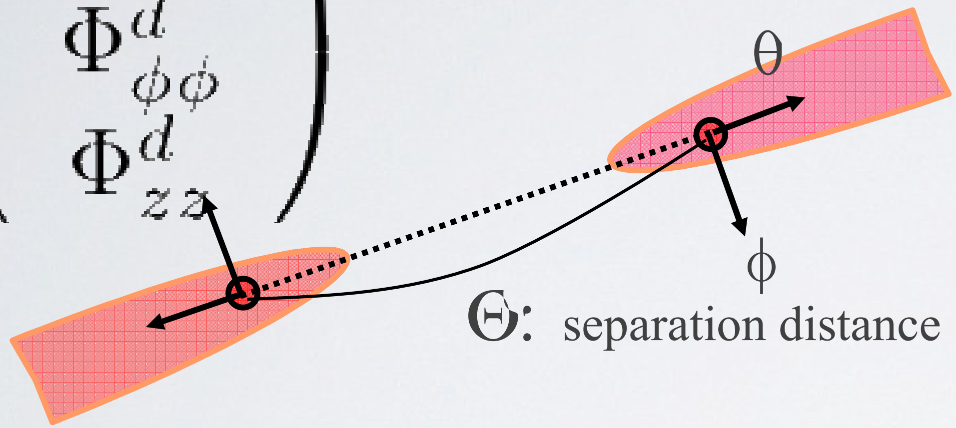

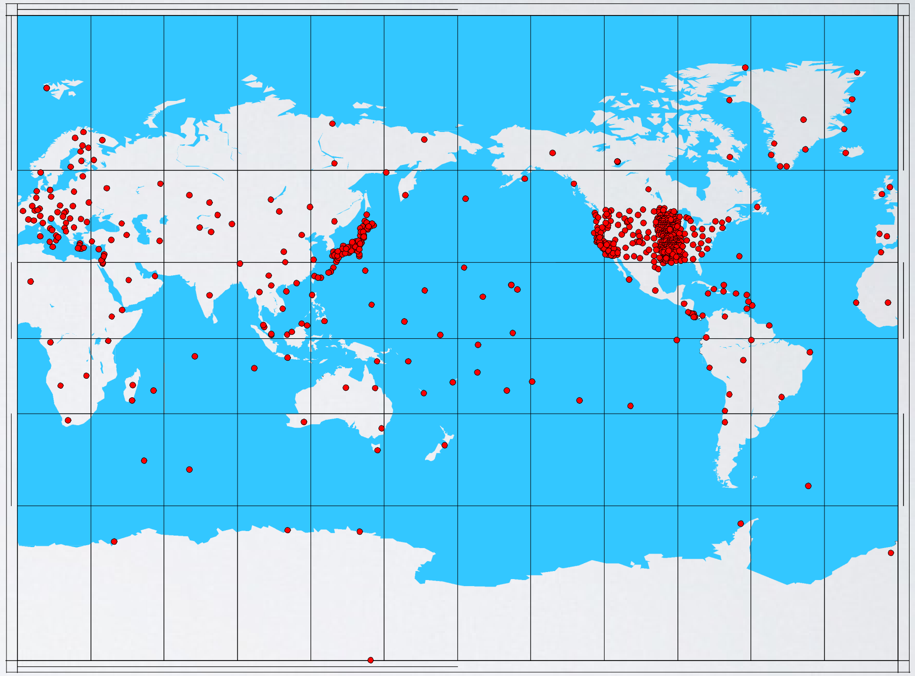

- Data: IRIS+ORFEUS+F-net STS1,2,2.5: 658 stations 2004/1-2011/12
- Exclusion of noisy data and effects of large earthquakes
- CCFs: radial-radial, transverse-transverse, and vertical-vertical

Wavenumber-frequency spectra

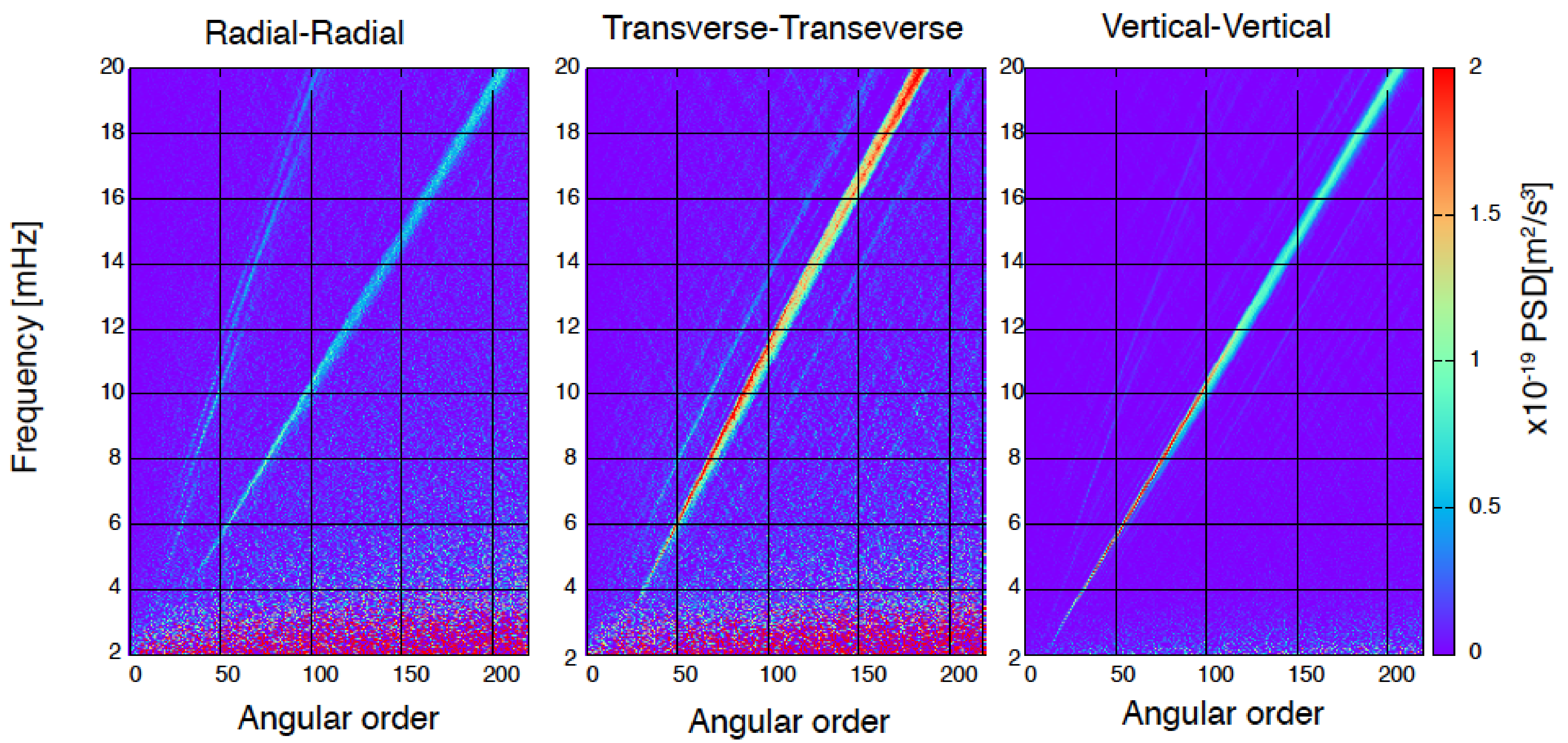

Assumptions of sources

- Stochastic source parameters
  - Power spectrum
  - Correlation length L

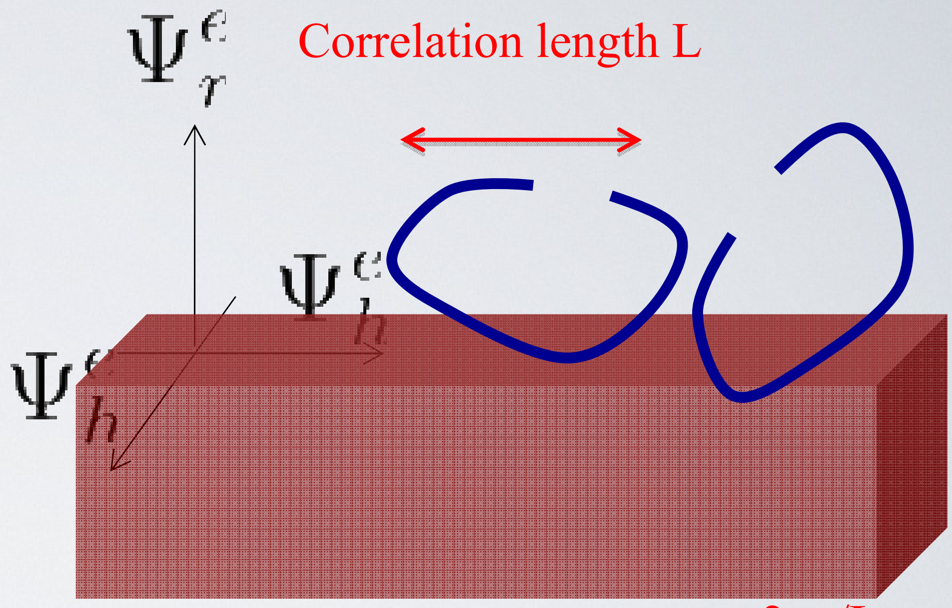

- Effective pressure and traction

Ψ_r^e Effective pressure

Ψ_h^e Effective traction

Power spectrum per unit wavenumber

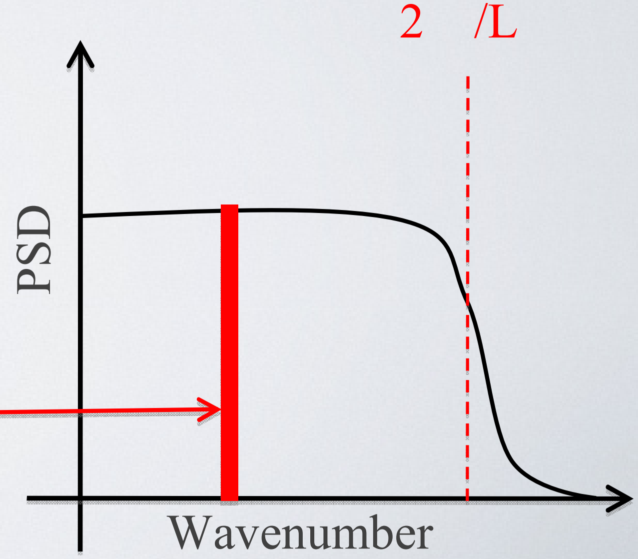

Inversion of source terms

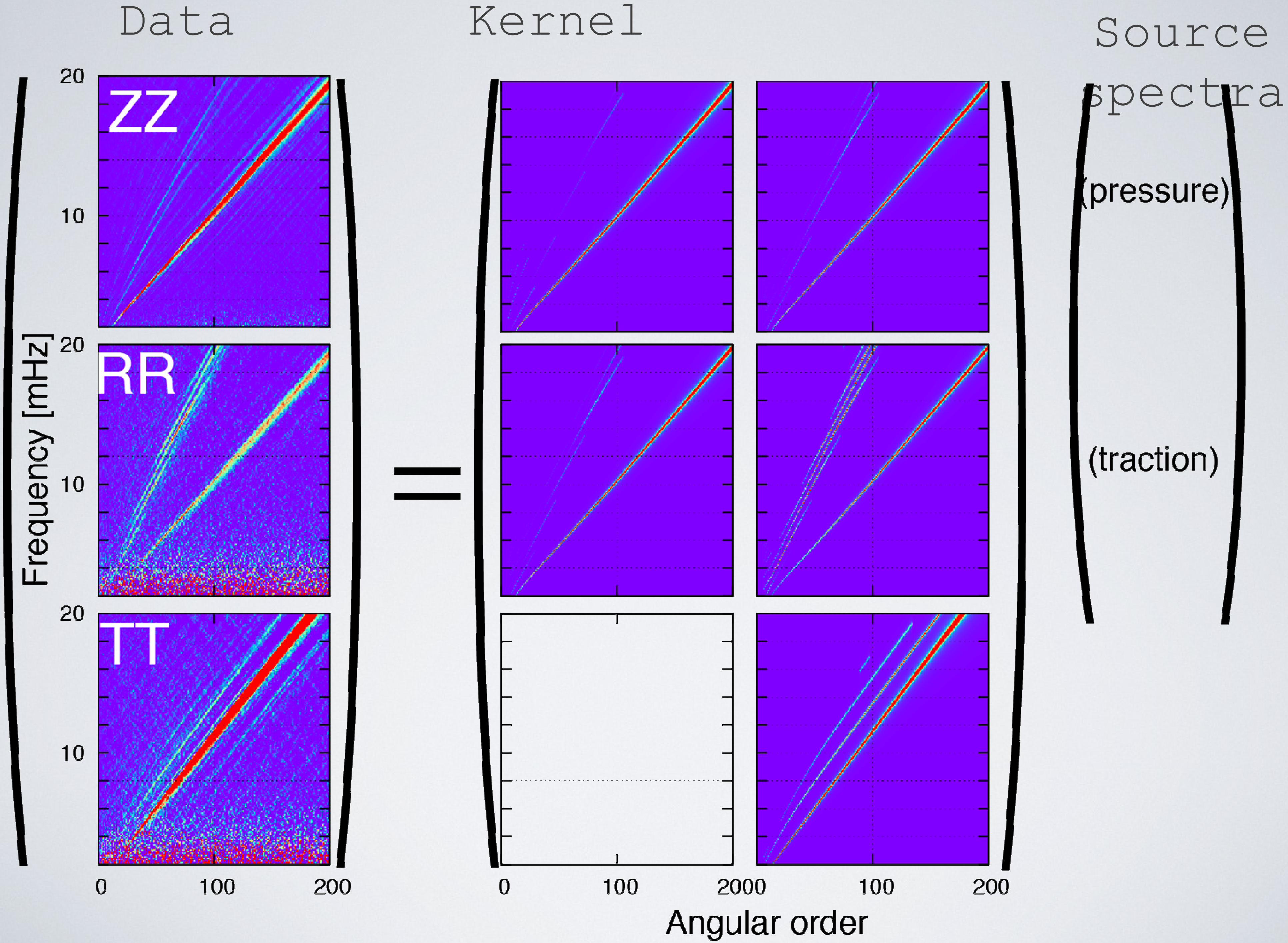

Estimated source spectra

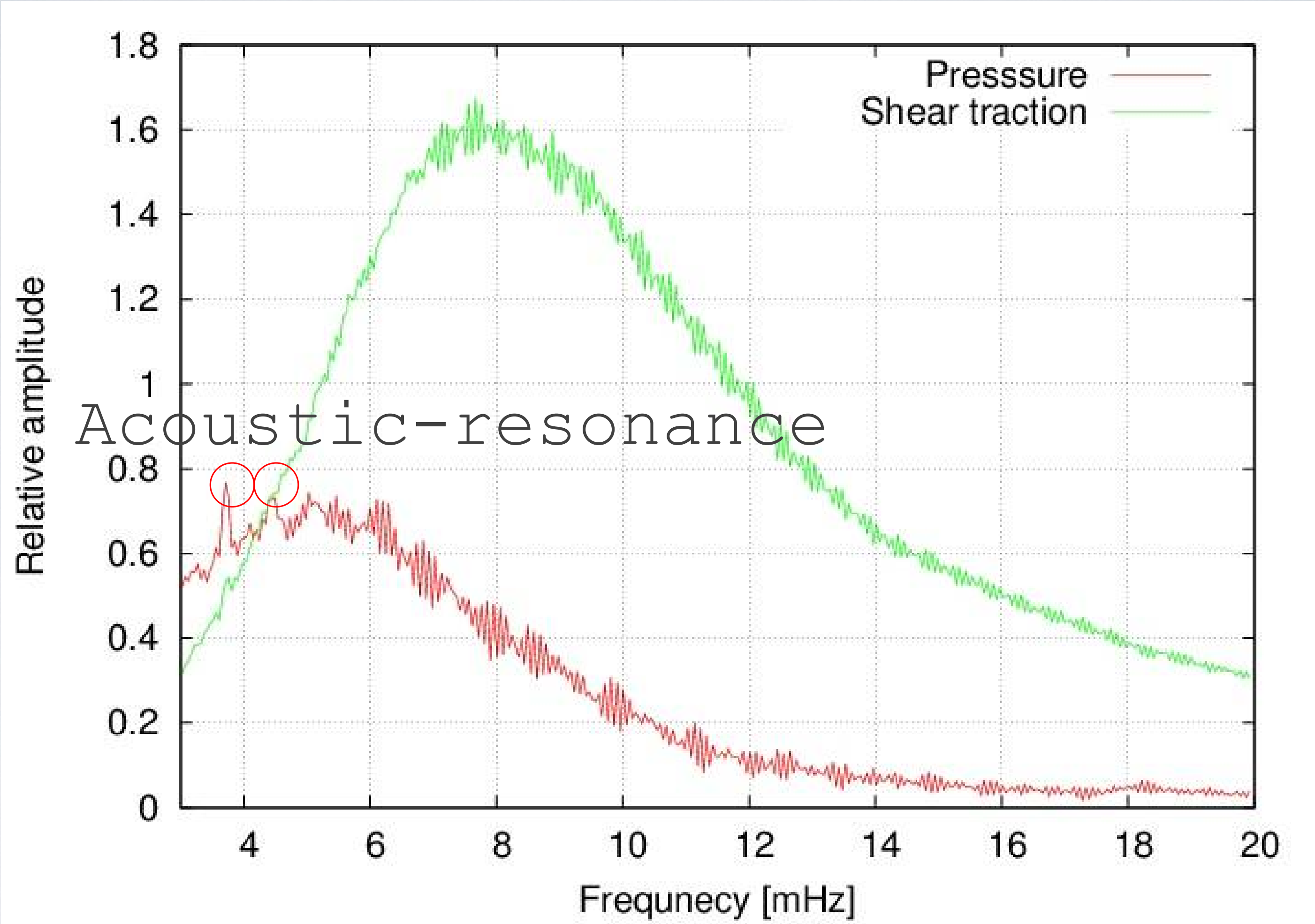

- Random shear traction: 5-20 mHz (a peak at 8 mHz)
- Pressure source: 2-5 mHz (a peak at 5 mHz)

Body wave propagation

P410P, P660P, *Poli et al 2012*
Core phases, *Lin et al* 2013

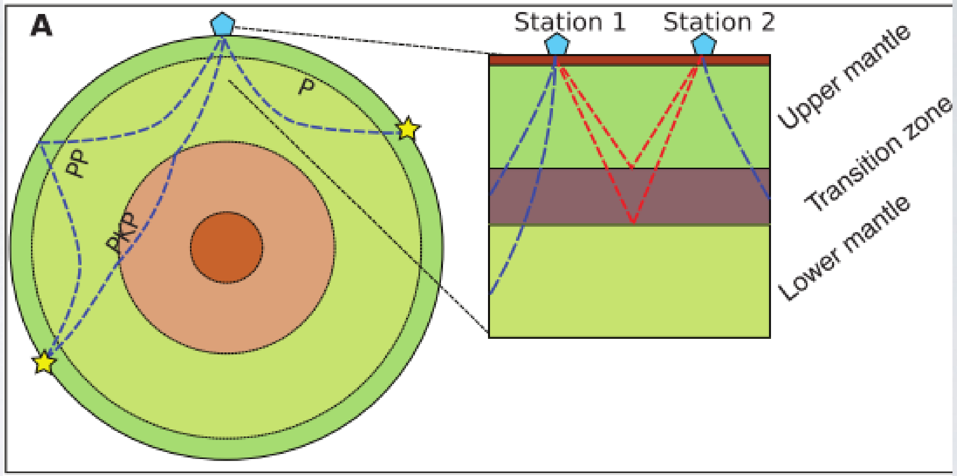

Lin et al 2013

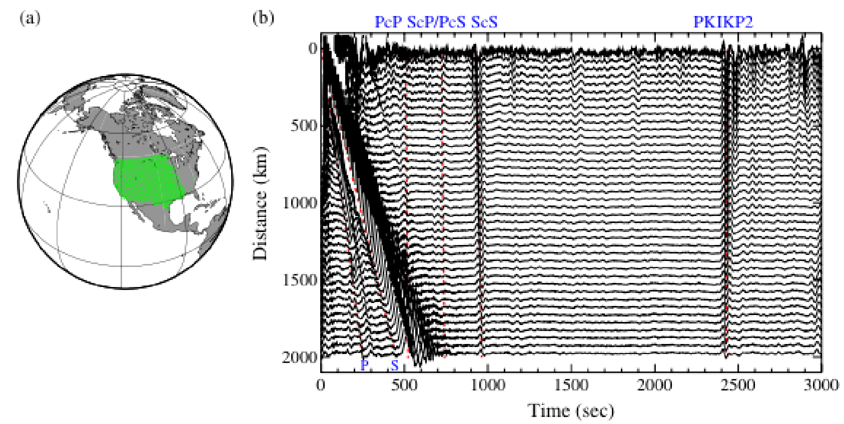

Figure 2. Stacked cross-correlations across USArray. (a) The USArray Transportable Array used in this study. Station locations are marked by green dots. (b) The observed broadband stacked cross-correlations sorted by distance. The red dashed lines mark the ray-predicted arrival times for core phases based on the iasp91 Earth model. Several observed body wave phases are indicated.

Poli et al 2012

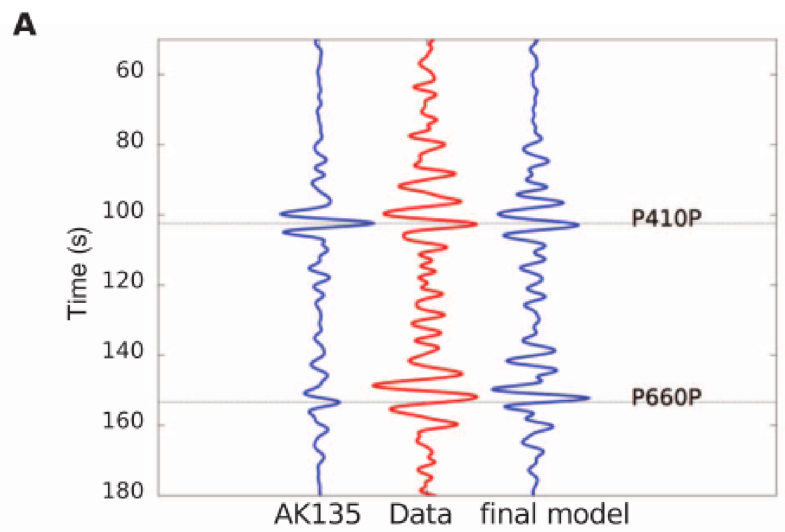

TRAVEL TIME PLOTS (CCFS)

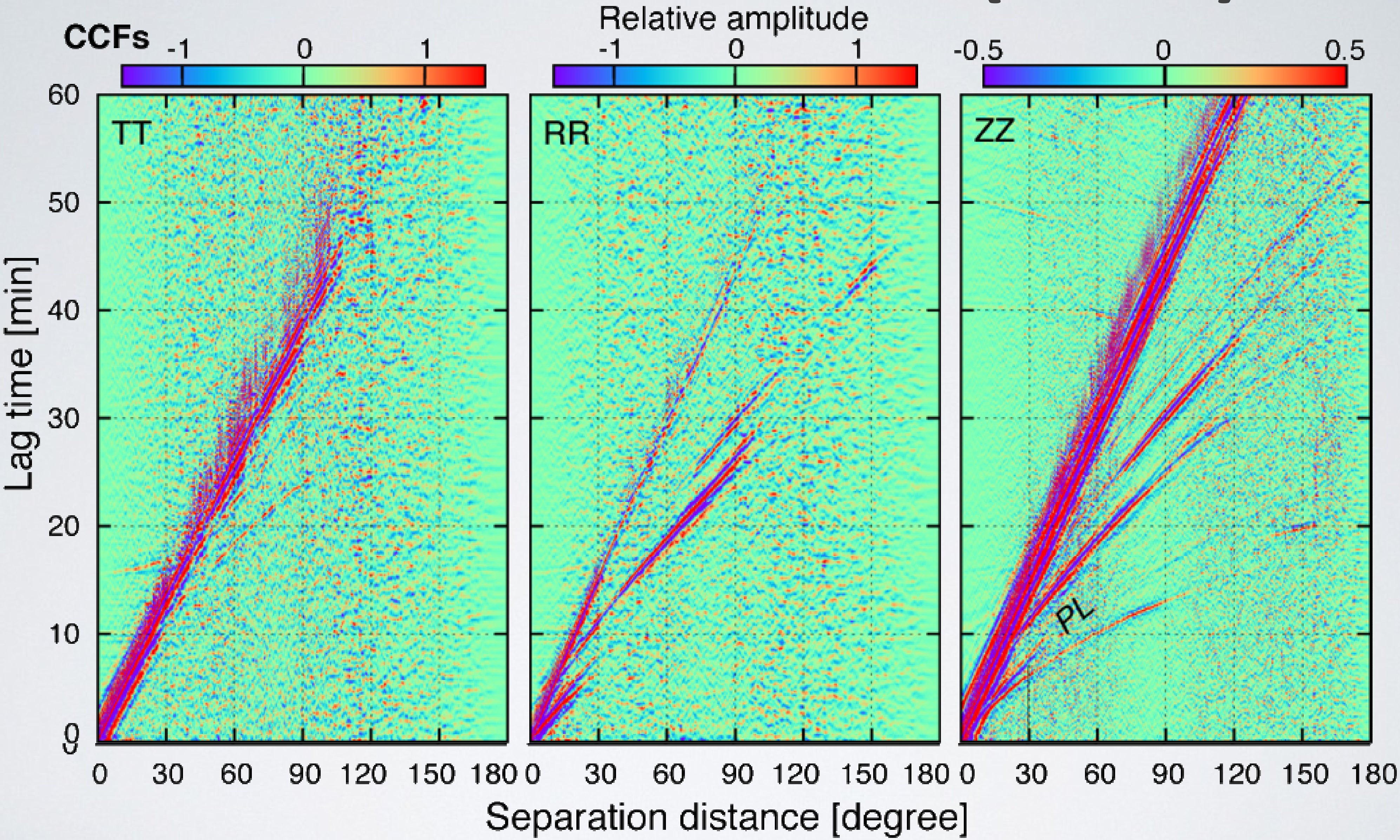

- Frequency range: 5-40 mHz
- Deconvolution by NLNM

Comparison of CCFs with Green's functions

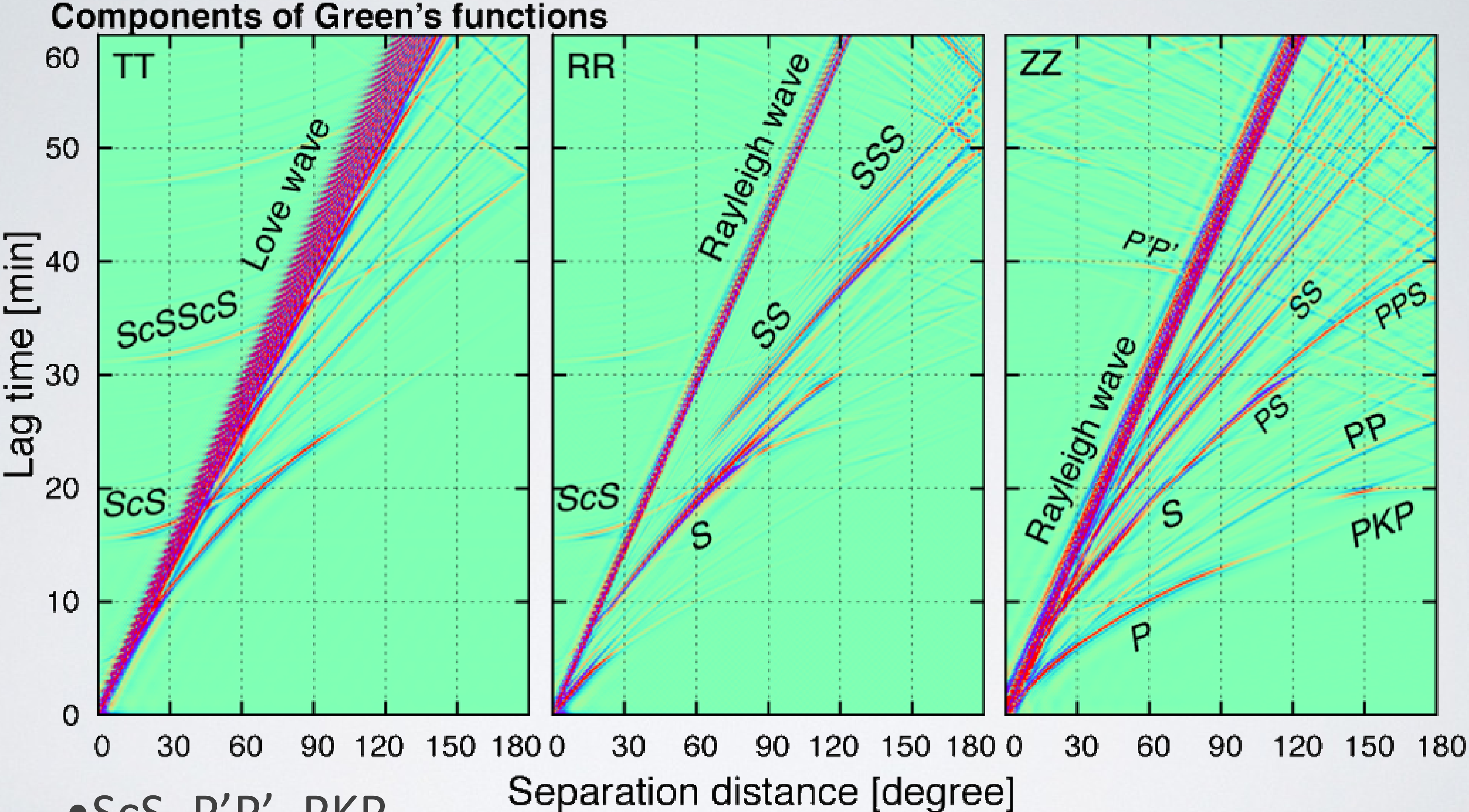

- ScS, P'P', PKP
- Lack of reflection phases in observation
- Dominance of Shear-coupled PL (SPL) wave

Dominance of SPL wave

The traction source radiates the strongest PL wave in the horizontal direction

PL wave couples with S wave

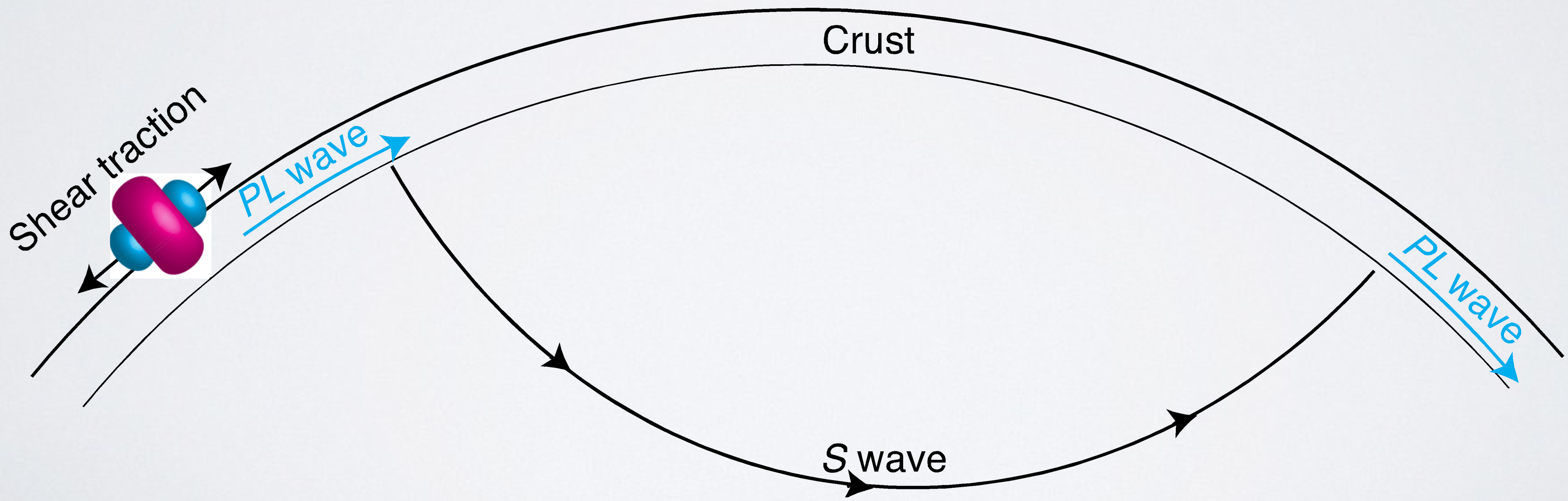

Synthetic seismograms

ZZ-component

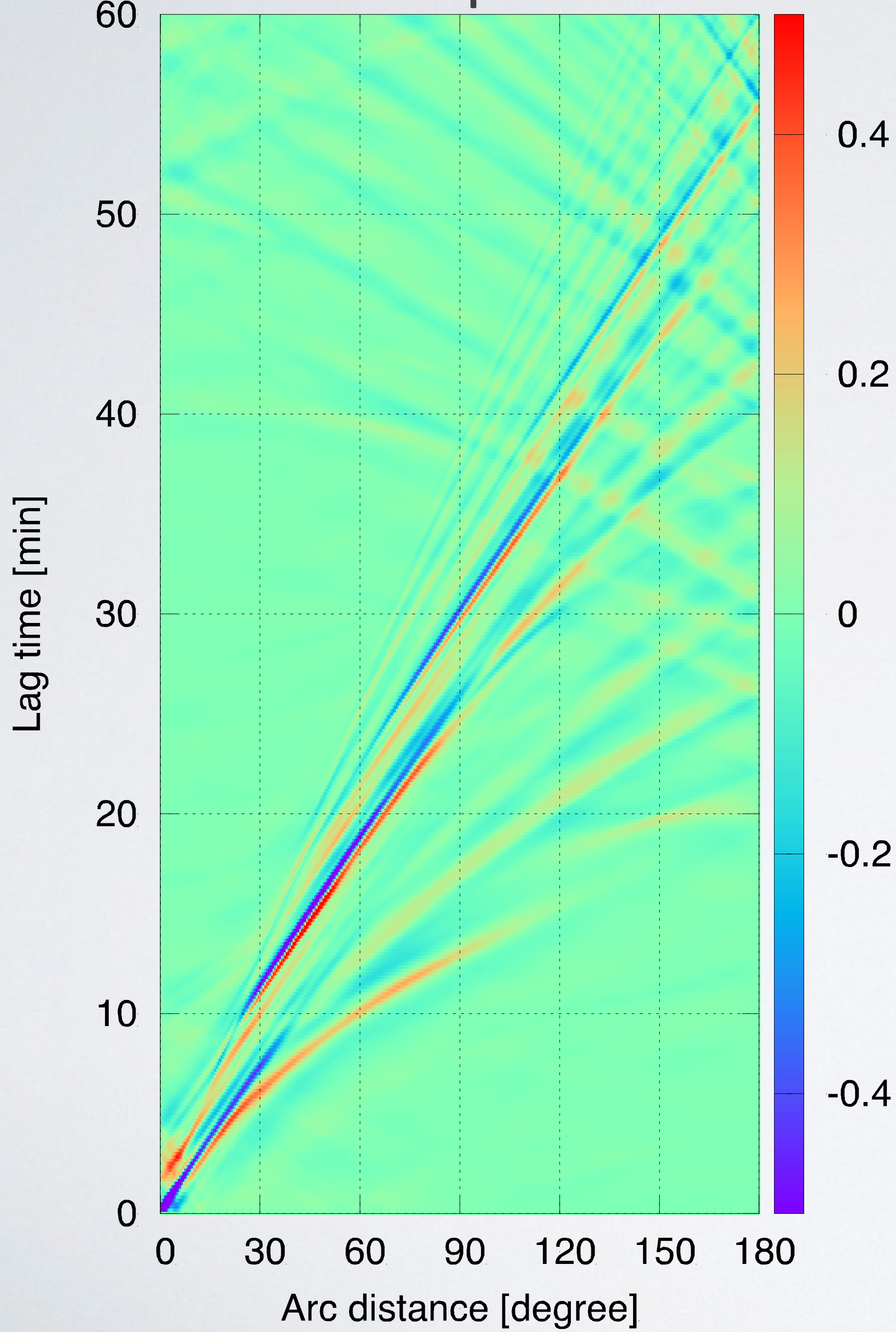

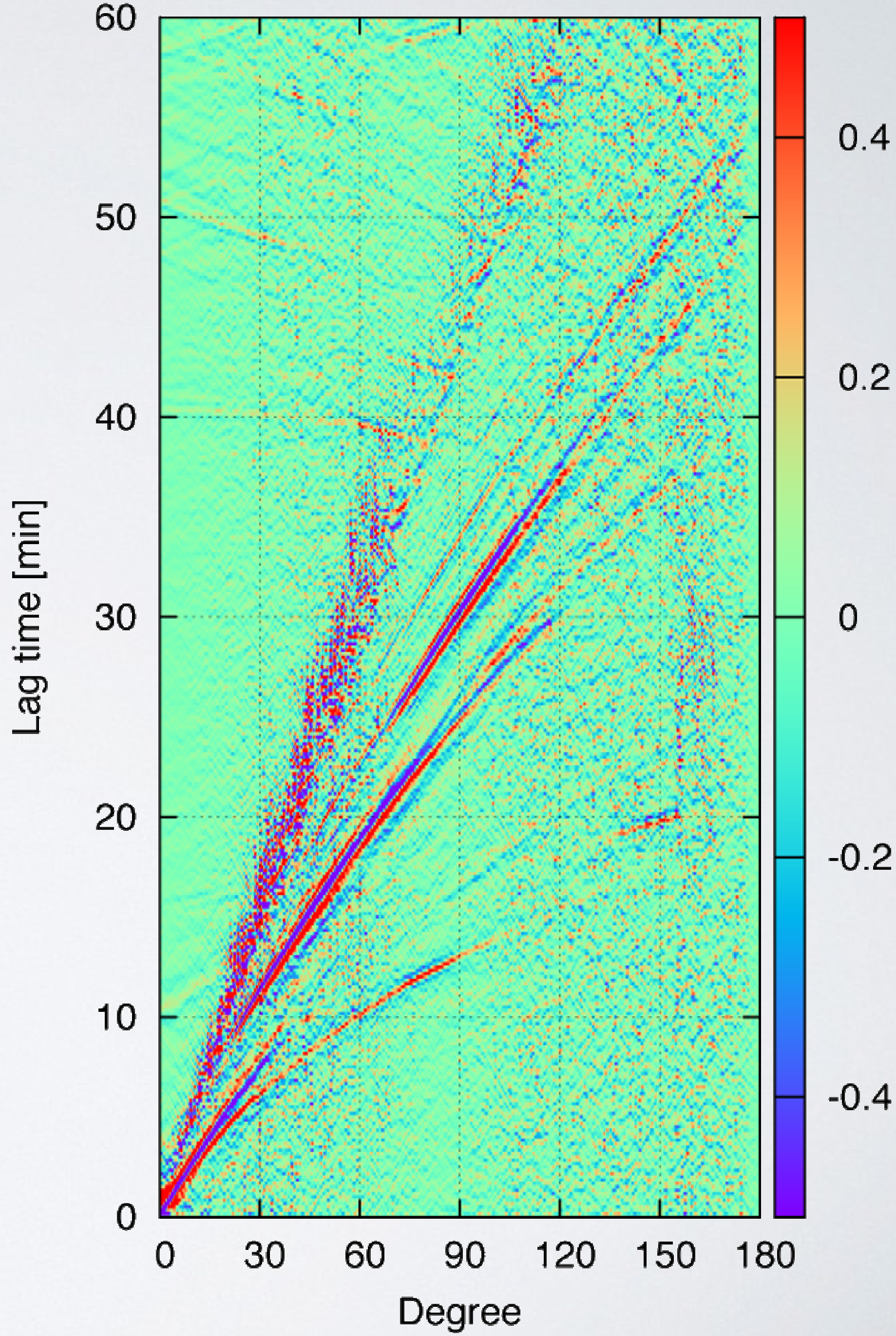

Conclusions

- Existence of background Love waves: from 3 mHz to 20 mHz
- Random surface traction is dominant above 5 mHz
- Linear topographic coupling on the ocean floor is the most probable excitation mechanism
- Below 5 mHz, additional pressure sources are needed
    - Atmospheric disturbances, and/or surf beat

Conclusions

- The CCFs show Global propagation of body waves
- Differences between the CCFs and the Green's functions
  (1) The lack of reflection phases in the CCFs : surface excitation sources
  (2) Dominance of SPL waves in the CCFs: shear-traction sources

End

Travel time anomalies (S and SS)

- S and SS waves: 5-30 mHz
- Phase difference between observation and synthetics
- Cross-correlation > 0.8

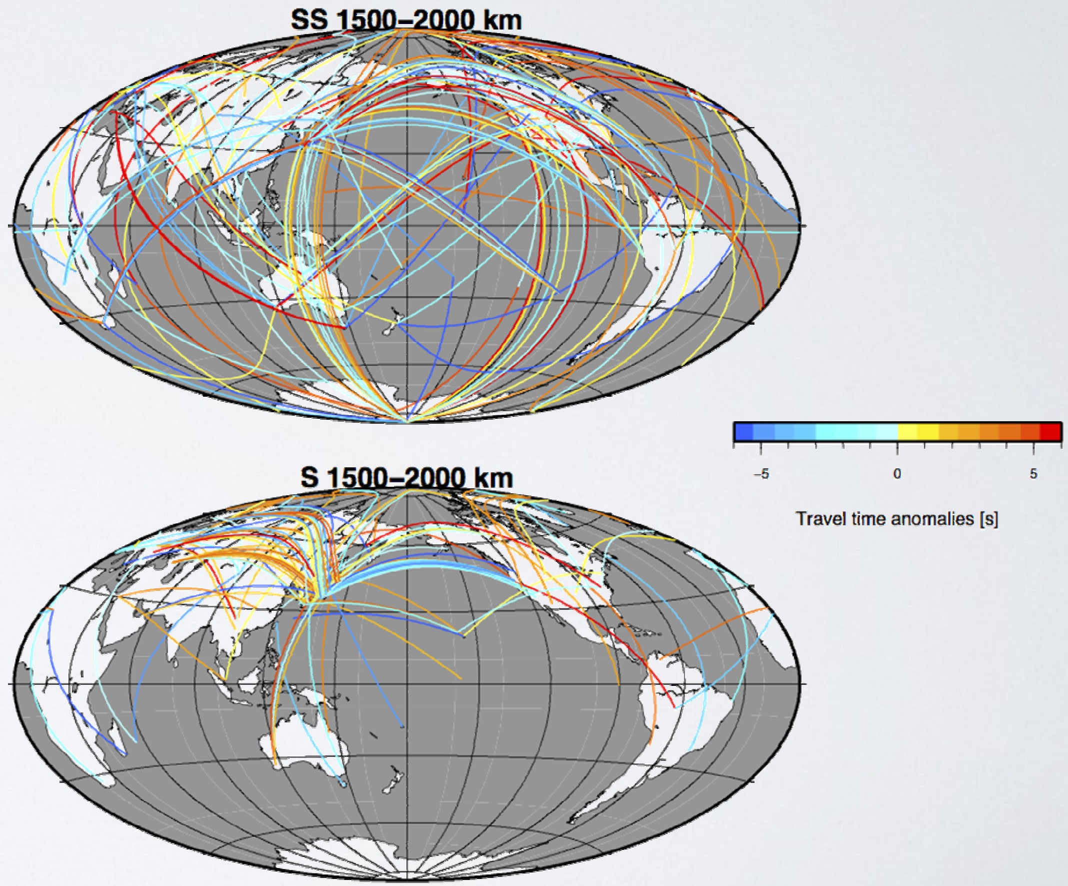

Body wave propagation revealed by ambient noise

- Local scale:
  - *e.g.* Roux 2005
- Regional scale:
  - *e.g.* Nishida *et al.* 2008, Poli *et al.* 2012
- High frequency (>0.5 Hz)

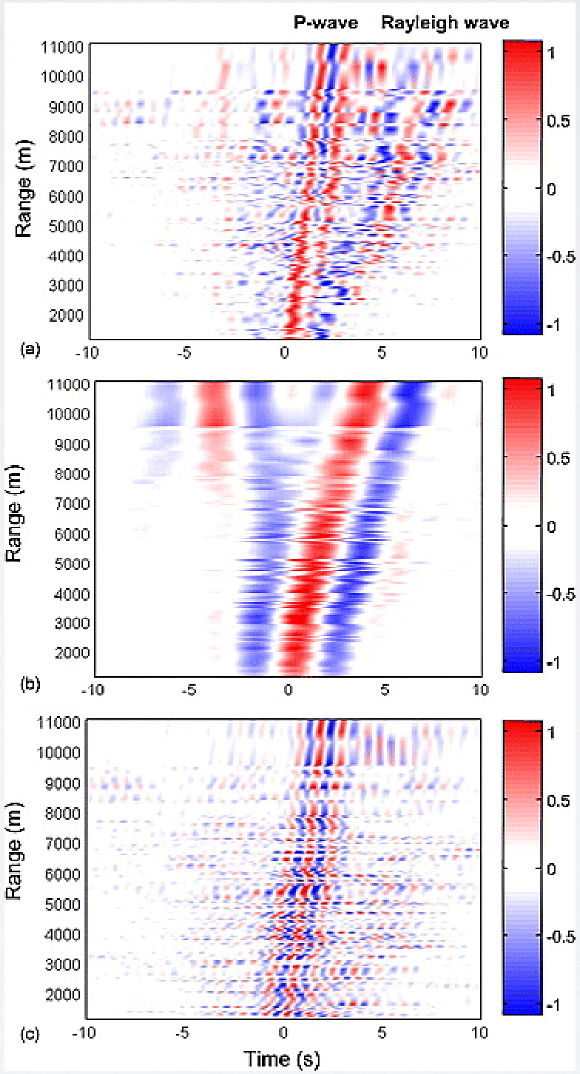

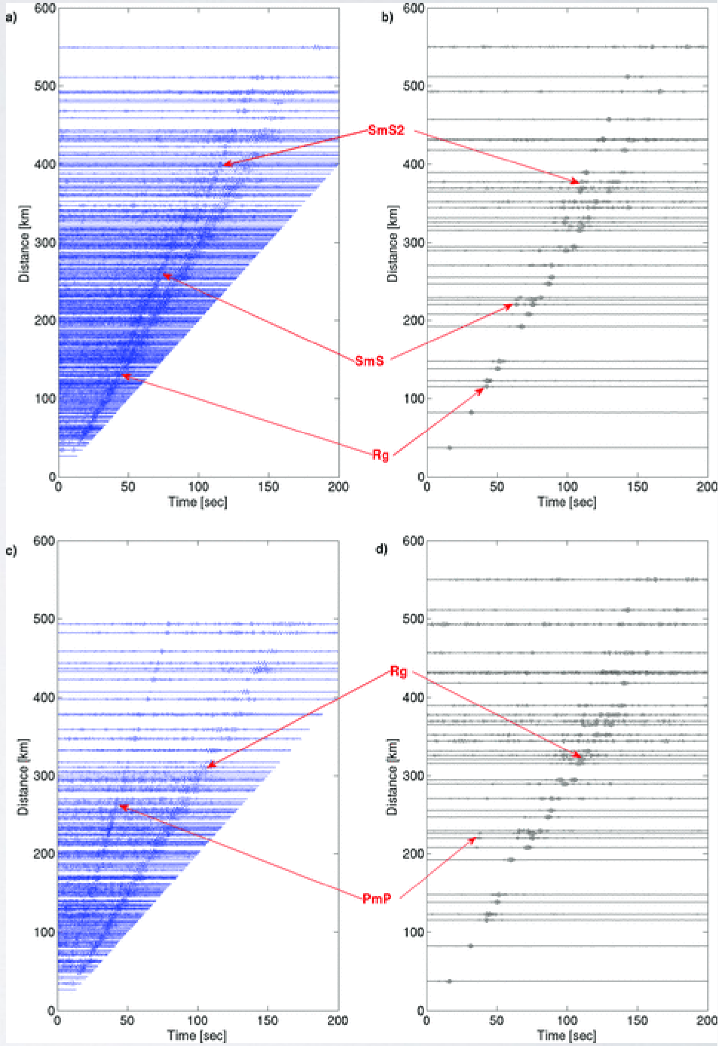

11 km: Roux 2005

600 km: Poli *et al.* 2

Excitation mechanism of seismic hum

Abyssal plane:

- Linear topographic coupling [Fukao et al, 2010; Saito, 2010]

Along a continental shelf:

- Surf beat: Nonlinear interactions

Atmospheric

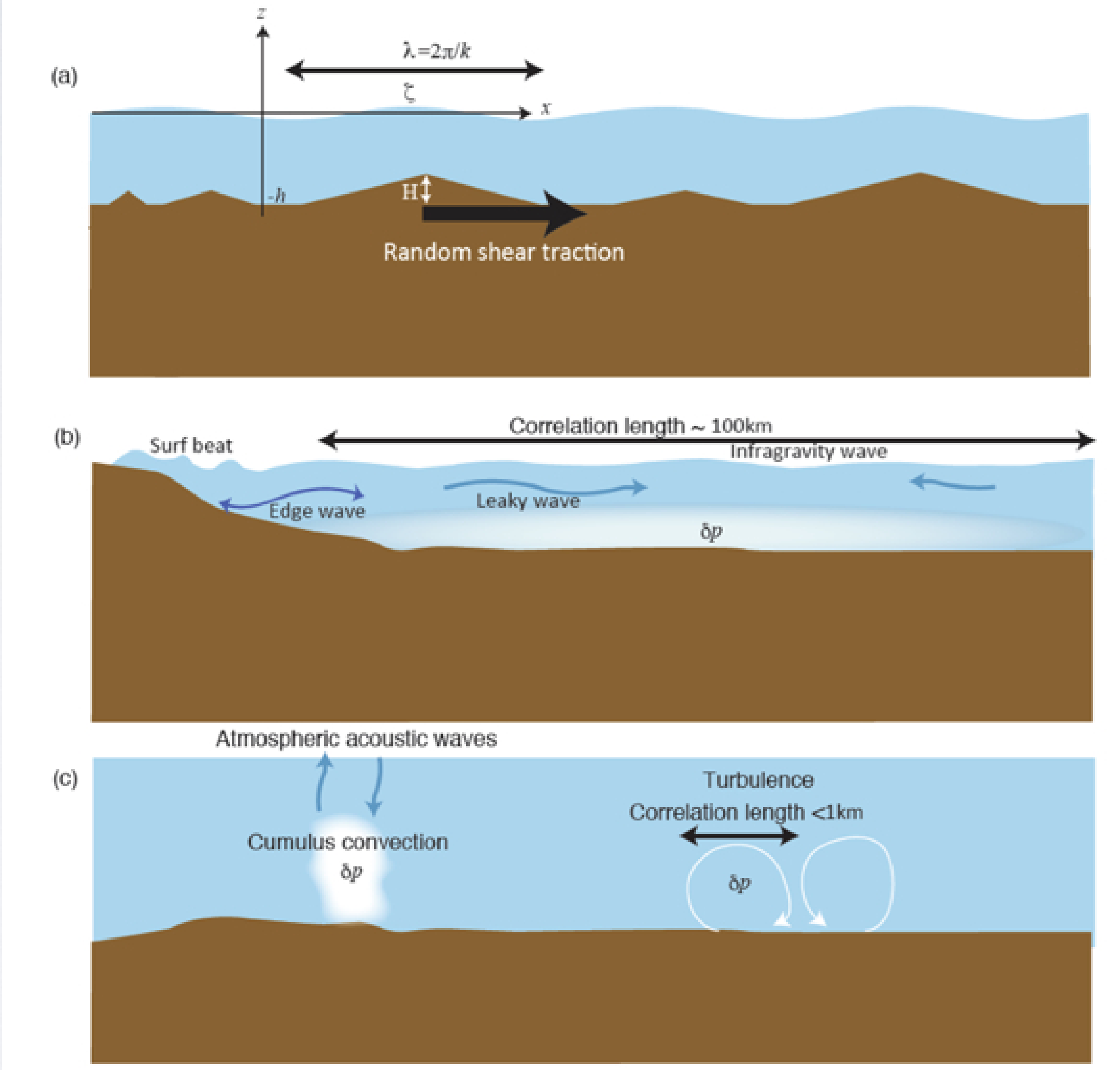

Nishida [2013]

The purpose of this study

- Determination of amplitudes of toroidal modes below 10 mHz
- To elucidate the force system of the excitation sources

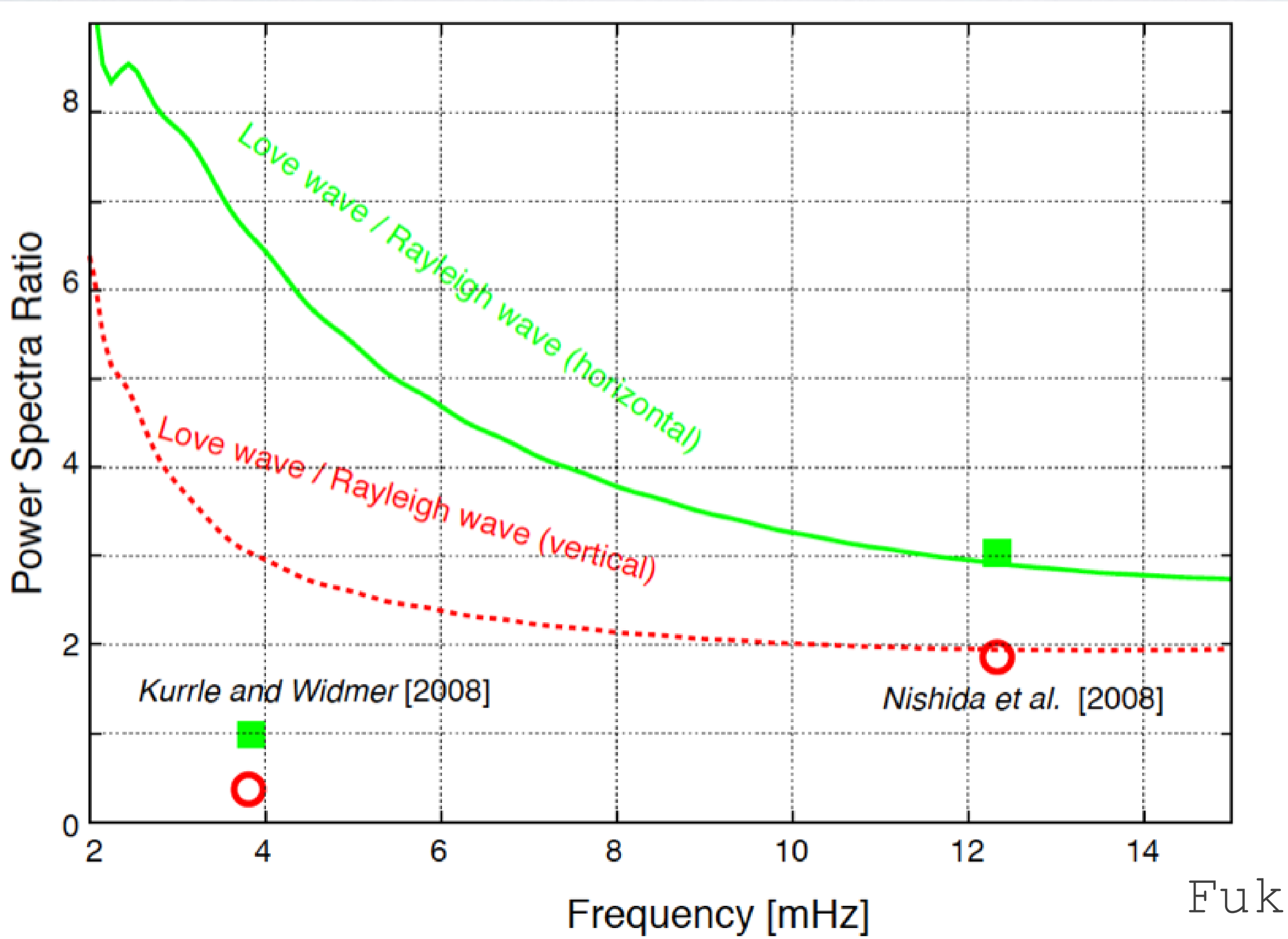

Fukao et al. (2010

Source distribution

- Source distribution
  - (1) Array observation
  - (2) Modeling of cross spectra
- Strong excitation
  - In the north Pacific in winter
  - In the southern hemisphere in summer
- Oceanic infragravity waves
  - Consistent with wave height data

Watada and Masters [2001] ,Rhie and Romonowicz [2004], Tanimoto [2005], Webb [2007]

(1)

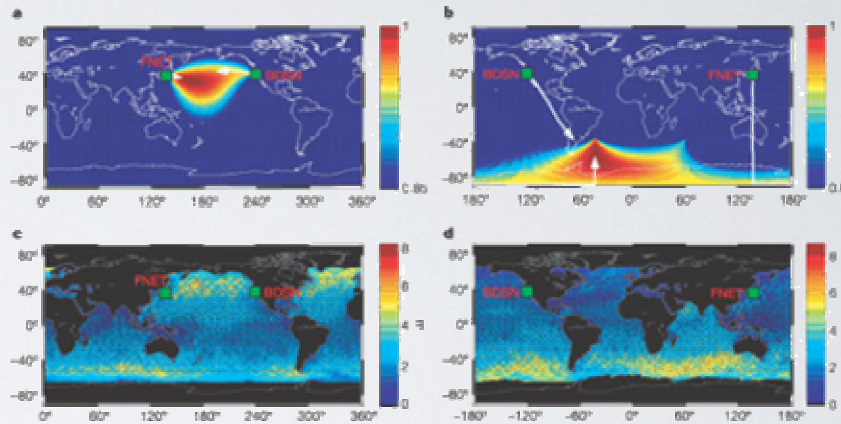

Rhie and Romonowicz [2004]

(2)

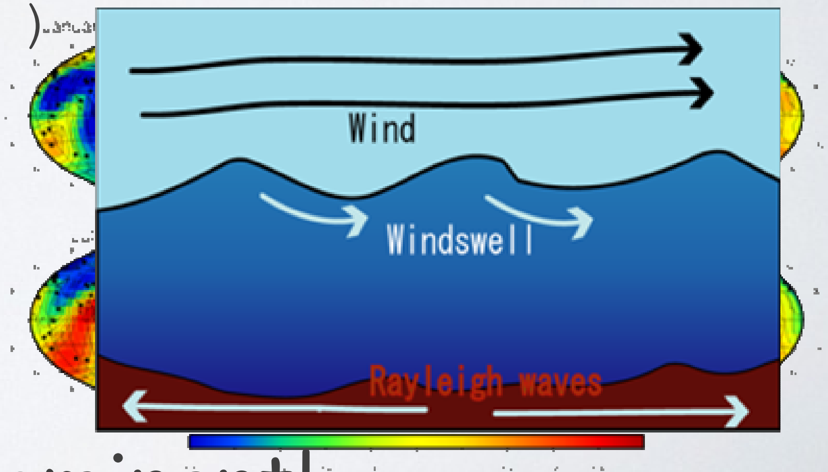

Anyway pressure sources are dominant!

Nishida and Fukao [2007]

Dominance of SPL wave

Lack of reflection phases

Dominance of Shear-coupled PL (SPL) wave

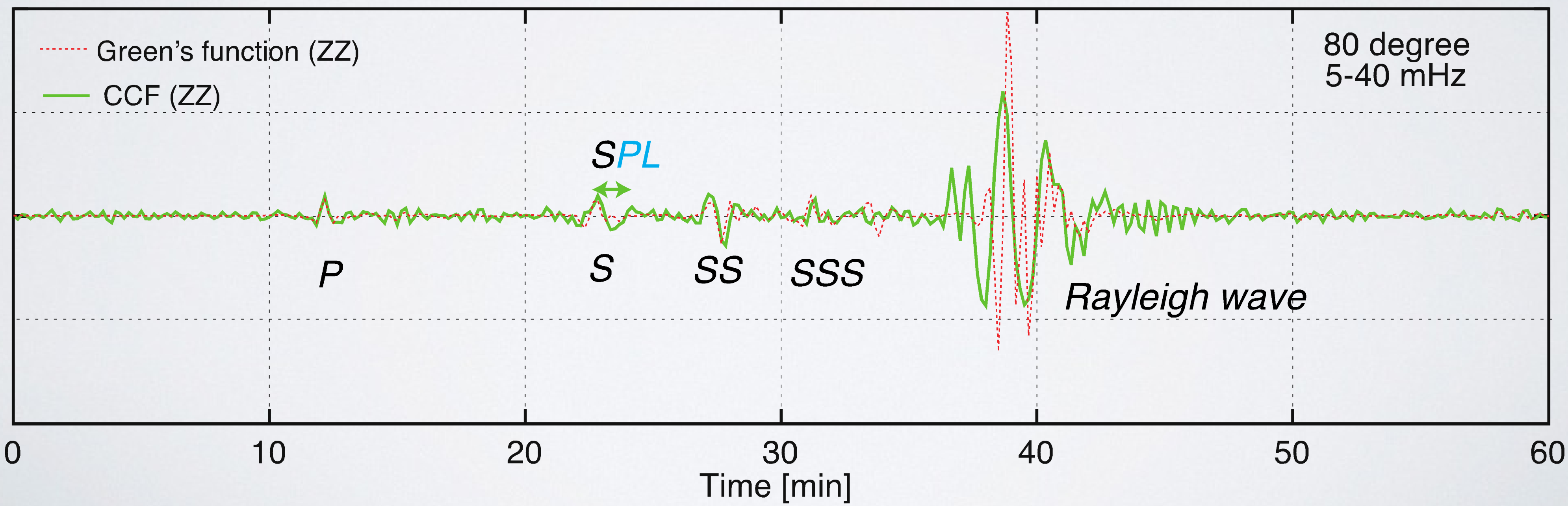

Conclusions

- Global propagation of body waves extracted by cross-correlation analysis of F-net, USArray, IRIS, FDSN, and ORFEUS data.
- The observed seismograms can be synthesized with an assumption of stochastic stationary excitation by random surface traction and random pressure sources.
- Travel time anomalies (S and SS) can be measured from phase difference between synthetic data and observed ones.

Acoustic resonance

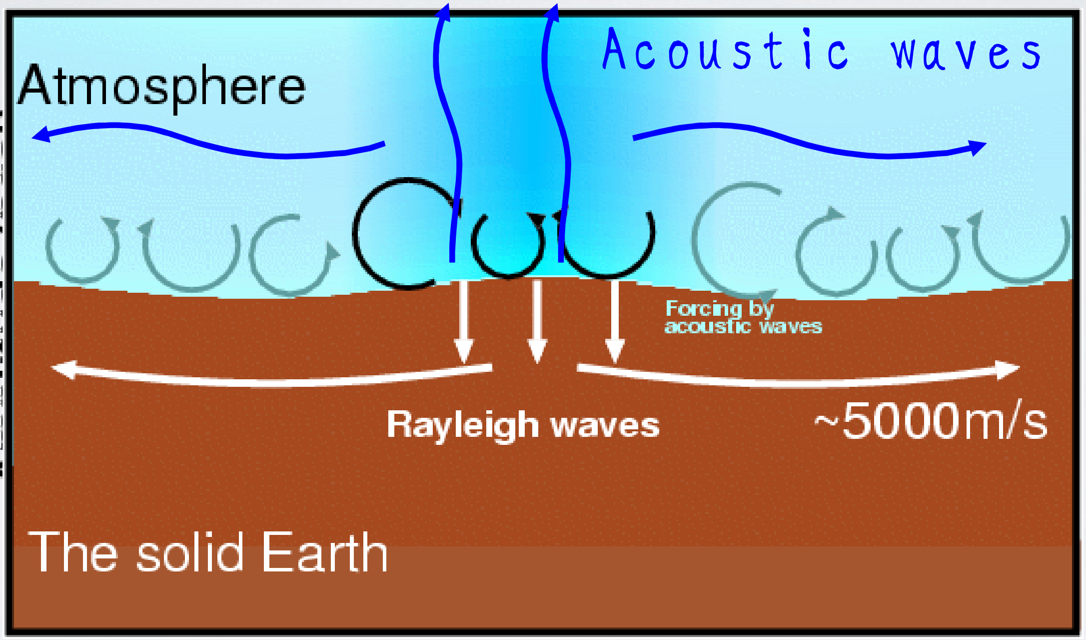

Mode number

Nishida et al. [2000]

- Excess amplitudes: $_0S_{29}$, $_0S_{37}$ (220, 270 s)
- Atmospheric turbulence < 5 mHz

SEASONAL VARIATIONS

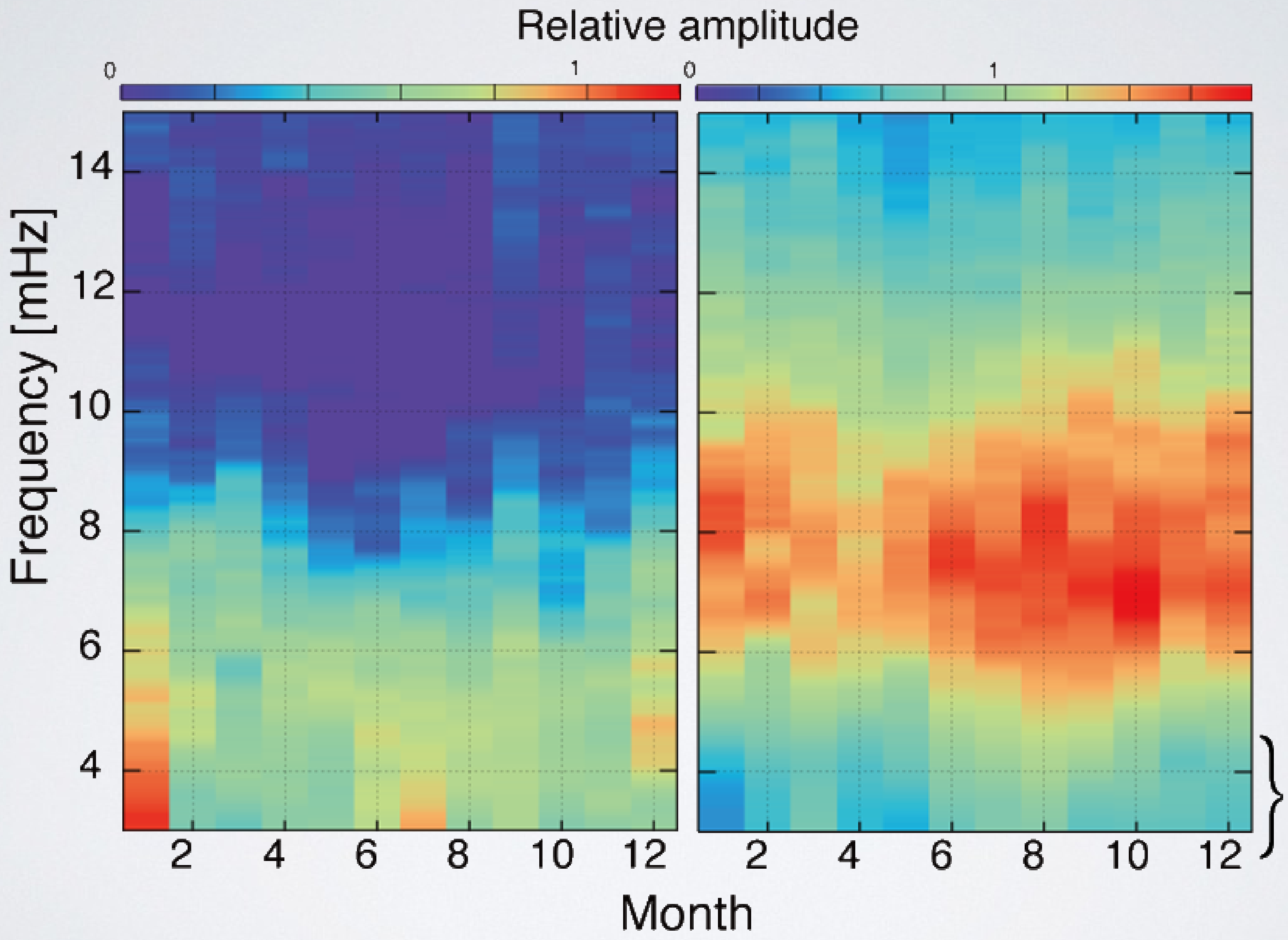

Fitting of cross spectra

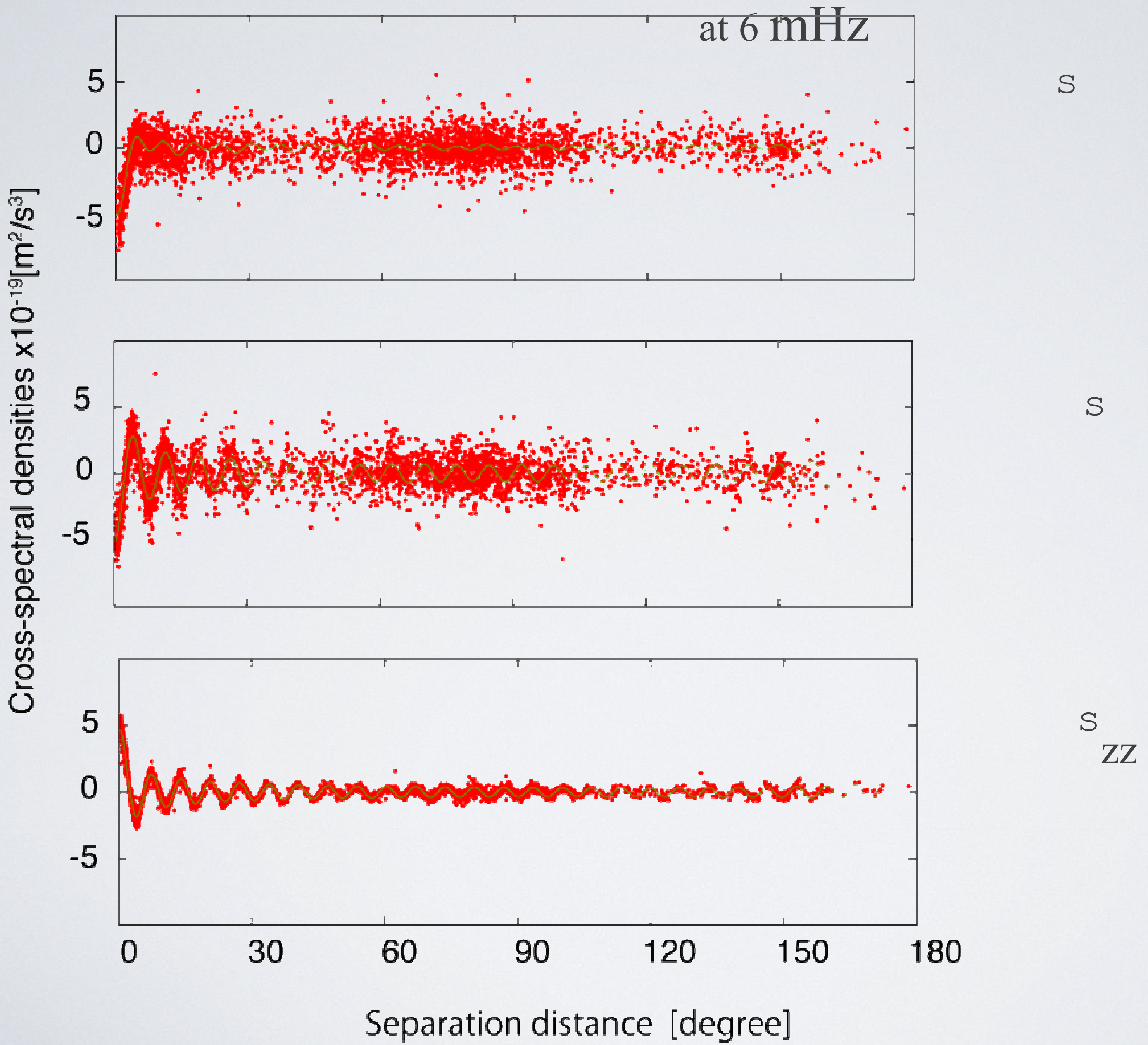

Travel time plots (CCFs)

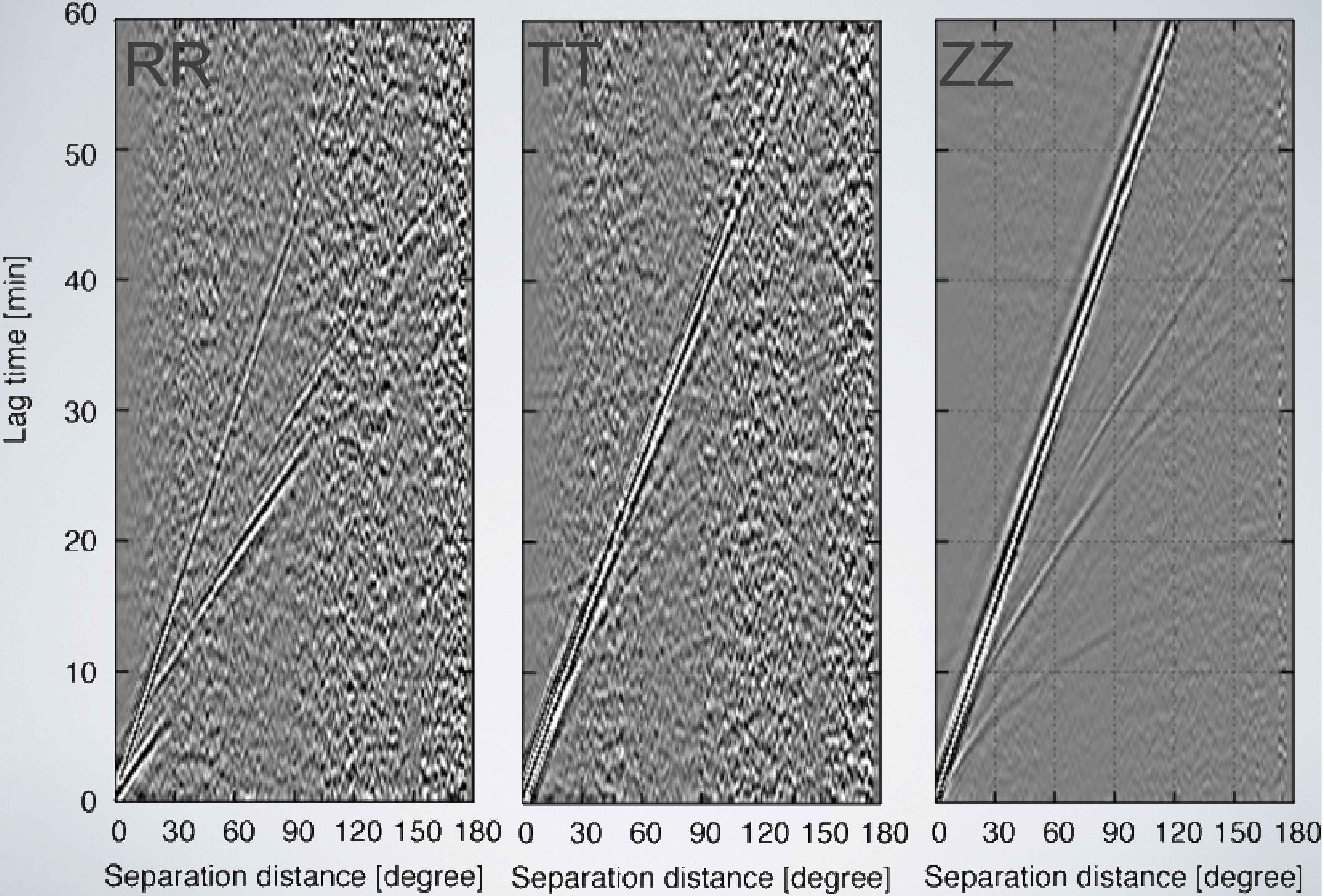

Synthetic cross-spectra

$$\Phi_{rr}(\Theta;\omega) = -R^2 \sum_l U_l^2 (\Psi_{rr}^e U_l^2 + \Psi_h^e V_l^2) \frac{2l+1}{4\pi l(l+1)} P_l(\cos\Theta) \left|\eta_l^R\right|^2 \quad (1)$$

$$\Phi_{\theta\theta}(\Theta;\omega) = -R^2 \sum_l V_l^2 (\Psi_{rr}^e U_l^2 + \Psi_h^e V_l^2) \frac{2l+1}{4\pi l(l+1)} \frac{d^2 P_l(\cos\Theta)}{d\Theta^2} \left|\eta_l^R\right|^2 \quad (2)$$

$$- R^2 \sum_l W_l^4 \Psi_h^e \frac{2l+1}{4\pi l(l+1)\sin\Theta} \frac{dP_l(\cos\Theta)}{d\Theta} \left|\eta_l^T\right|$$

$$\Phi_{\phi\phi}(\Theta;\omega) = -R^2 \sum_l V_l^2 (\Psi_{rr}^e U_l^2 + \Psi_h^e V_l^2) \frac{2l+1}{4\pi l(l+1)\sin\Theta} \frac{dP_l(\cos\Theta)}{d\Theta} \left|\eta_l^R\right|^2 \quad (3)$$

$$- R^2 \sum_l W_l^4 \Psi_h^e \frac{2l+1}{4\pi l(l+1)} \frac{d^2 P_l(\cos\Theta)}{d\Theta^2} \left|\eta_l^T\right|^2$$

$$\begin{pmatrix} \Phi^s_{\theta\theta}(\Theta,\Phi) \\ \Phi^s_{\phi\phi}(\Theta,\Phi) \\ \Phi^s_{zz}(\Theta,\Phi) \end{pmatrix} = \begin{pmatrix} K_{\theta r}(\Theta,\Phi) & K_{\theta h}(\Theta,\Phi) \\ K_{\phi r}(\Theta,\Phi) & K_{\phi h}(\Theta,\Phi) \\ K_{zr}(\Theta,\Phi) & K_{zh}(\Theta,\Phi) \end{pmatrix} \begin{pmatrix} \Psi_r \\ \Psi_h \end{pmatrix}$$

Cross-correlation analysis

Cross spectra

$$\begin{pmatrix} \Phi^d_{\theta\theta} \\ \Phi^d_{\phi\phi} \\ \Phi^d_{zz} \end{pmatrix}$$

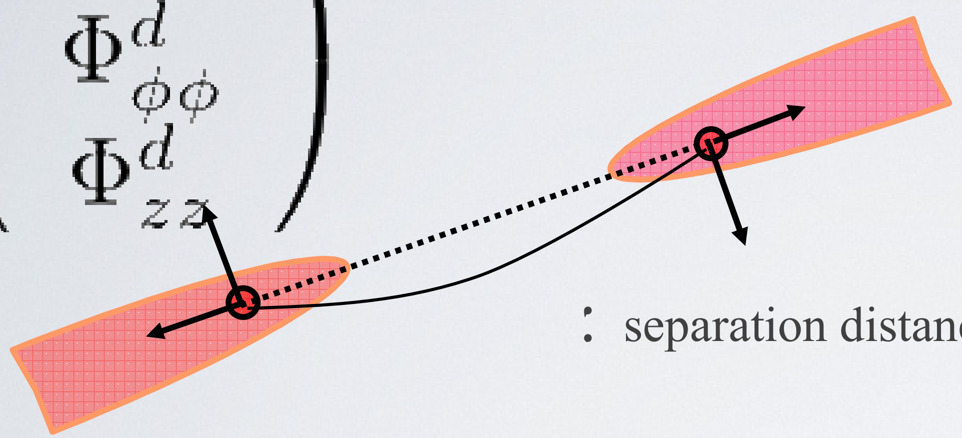

: separation distance

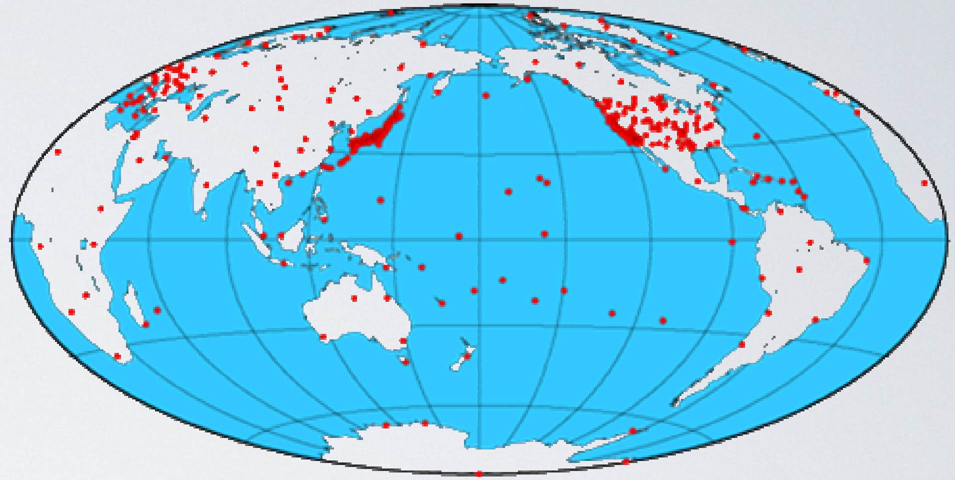

- Data: IRIS+ORFEUS+F-net STS1,2,2.5: 349 stations 2004/1-2011/12
- Cross spectra: radial-radial, transverse-transverse, and vertical-vertical

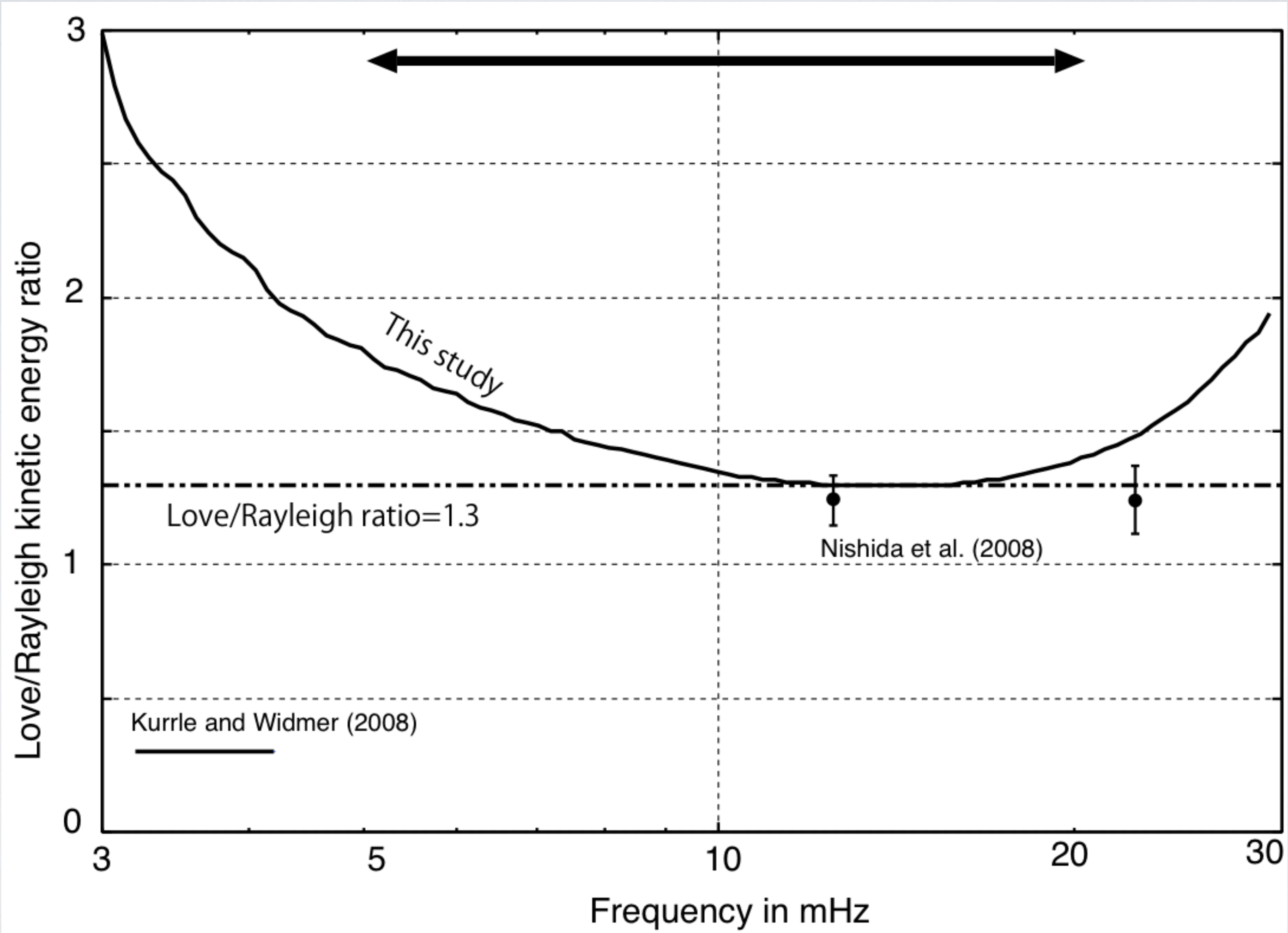

Fukao et al, 2010

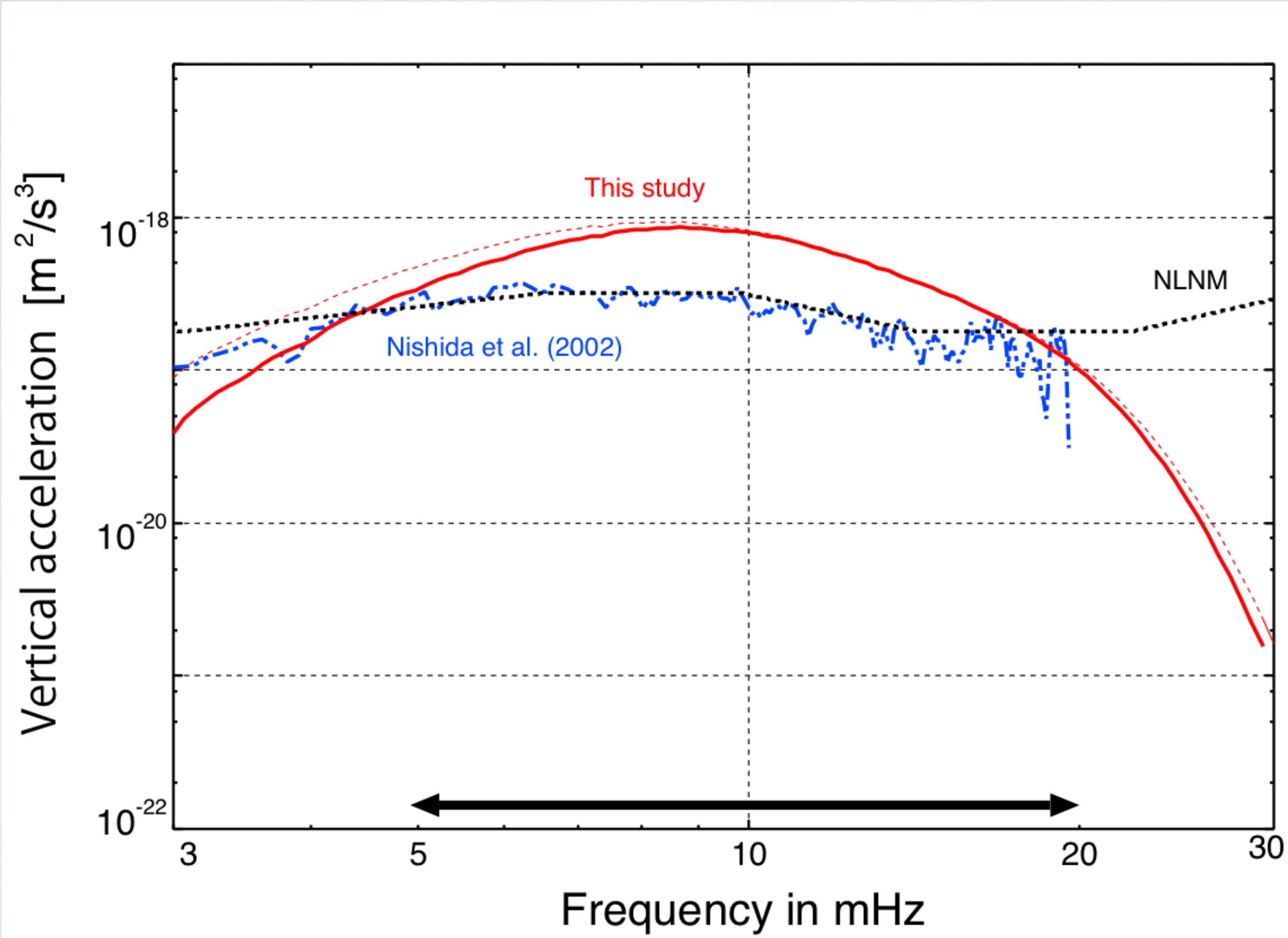

Fukao et al, 2010

Discovery of Earth's background free oscillations

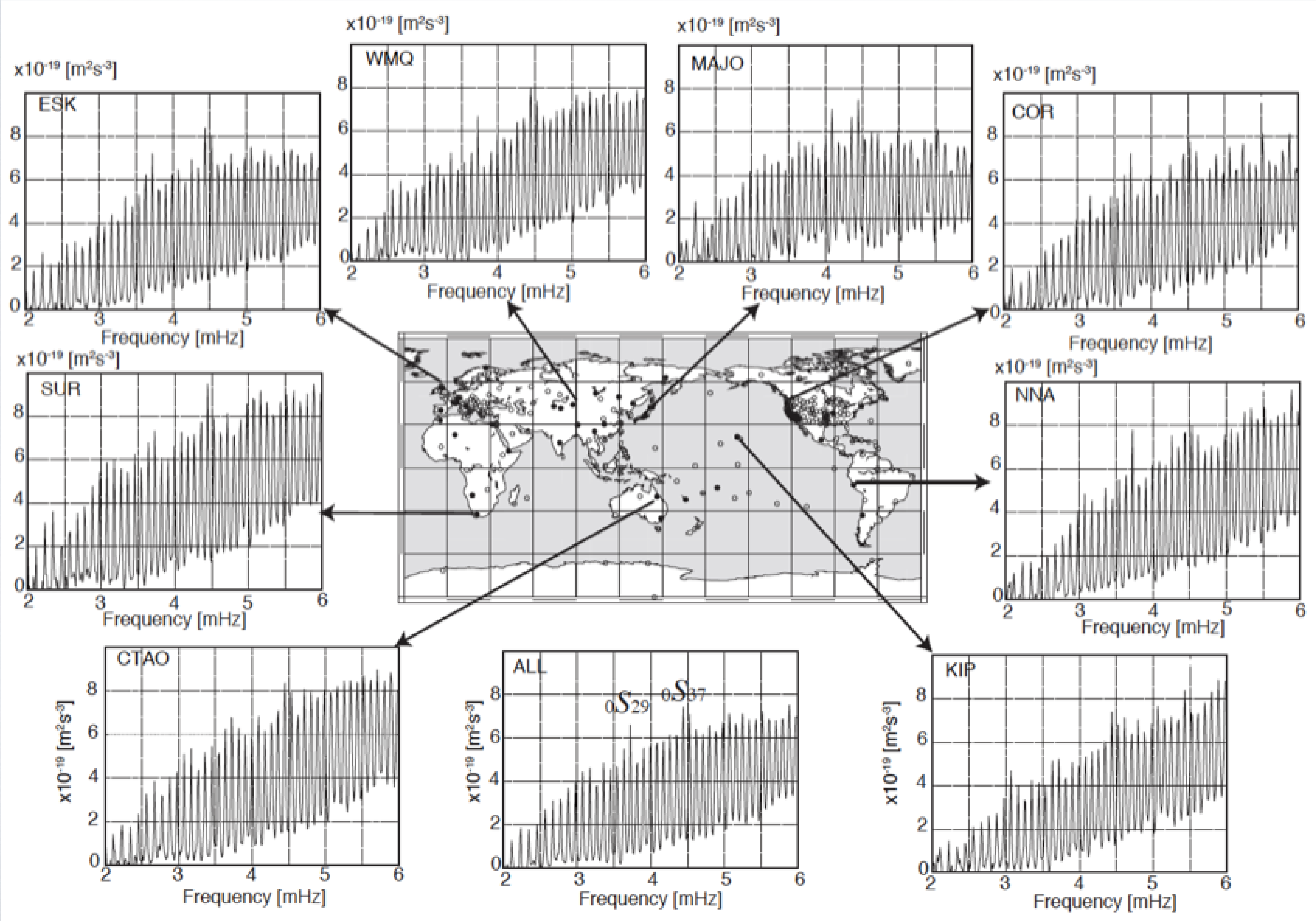

Slant stack analysis

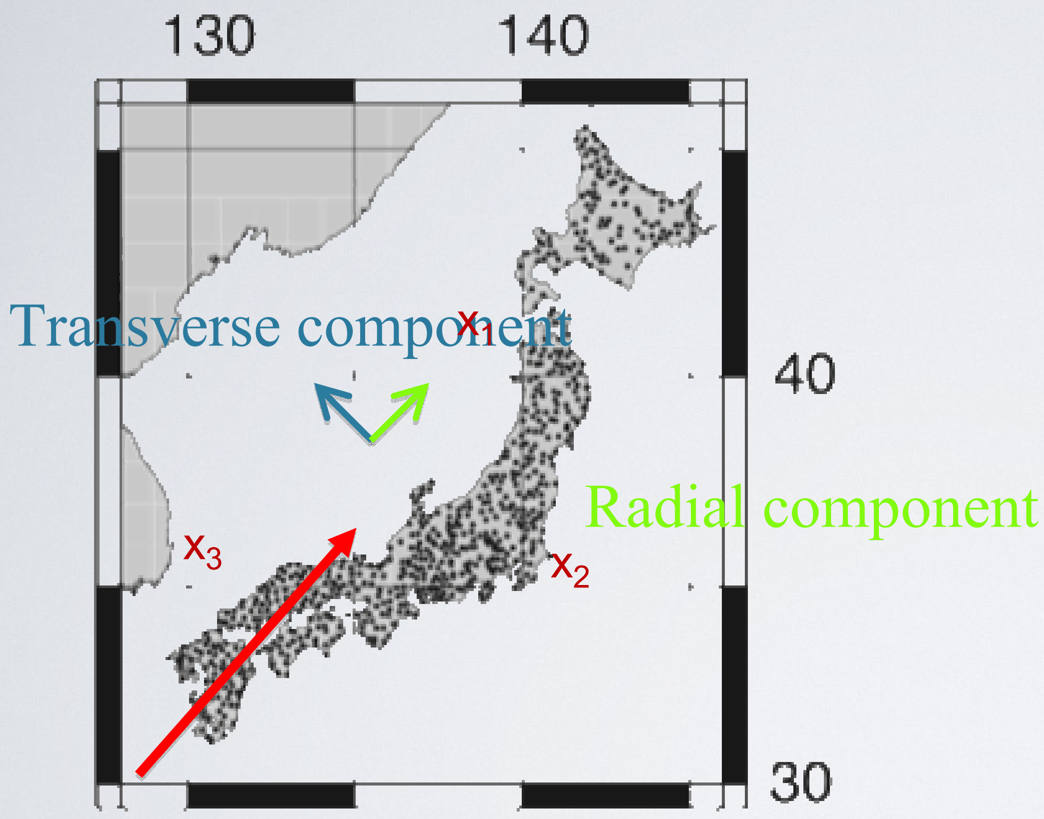

Slowness vector p

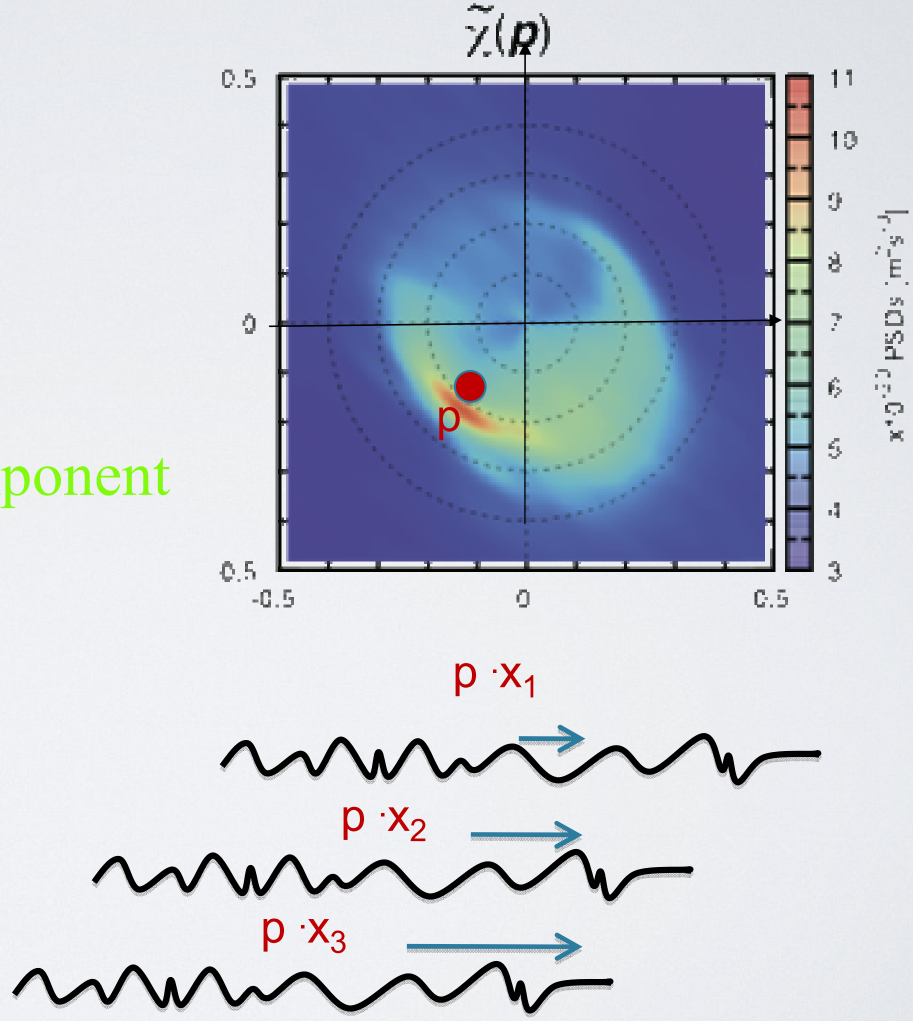

Noise level

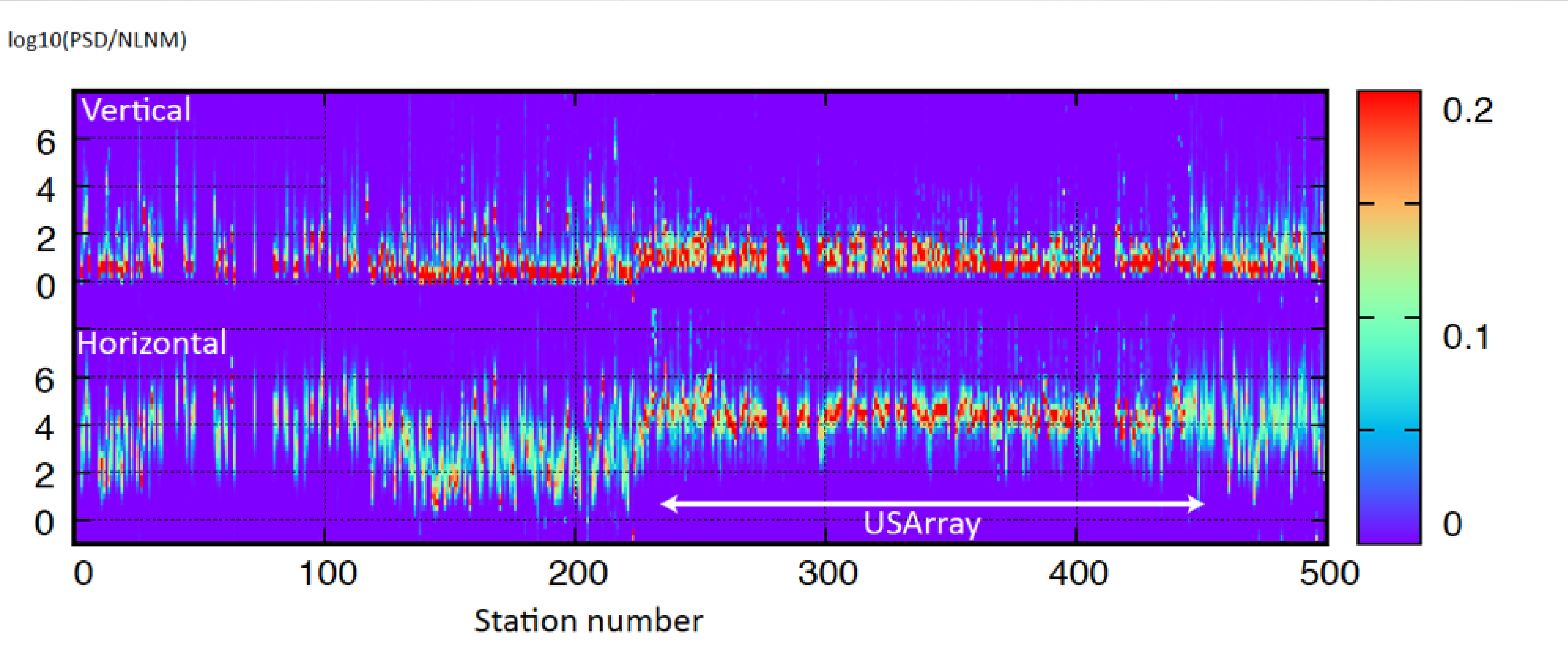

log10(PSD/NLNM)
Vertical
Horizontal
6
4
2
0
USArray
0
100
200
300
400
500
Station number
0.2
0.1
0

Resonance of infragravity wave with seafloor topography

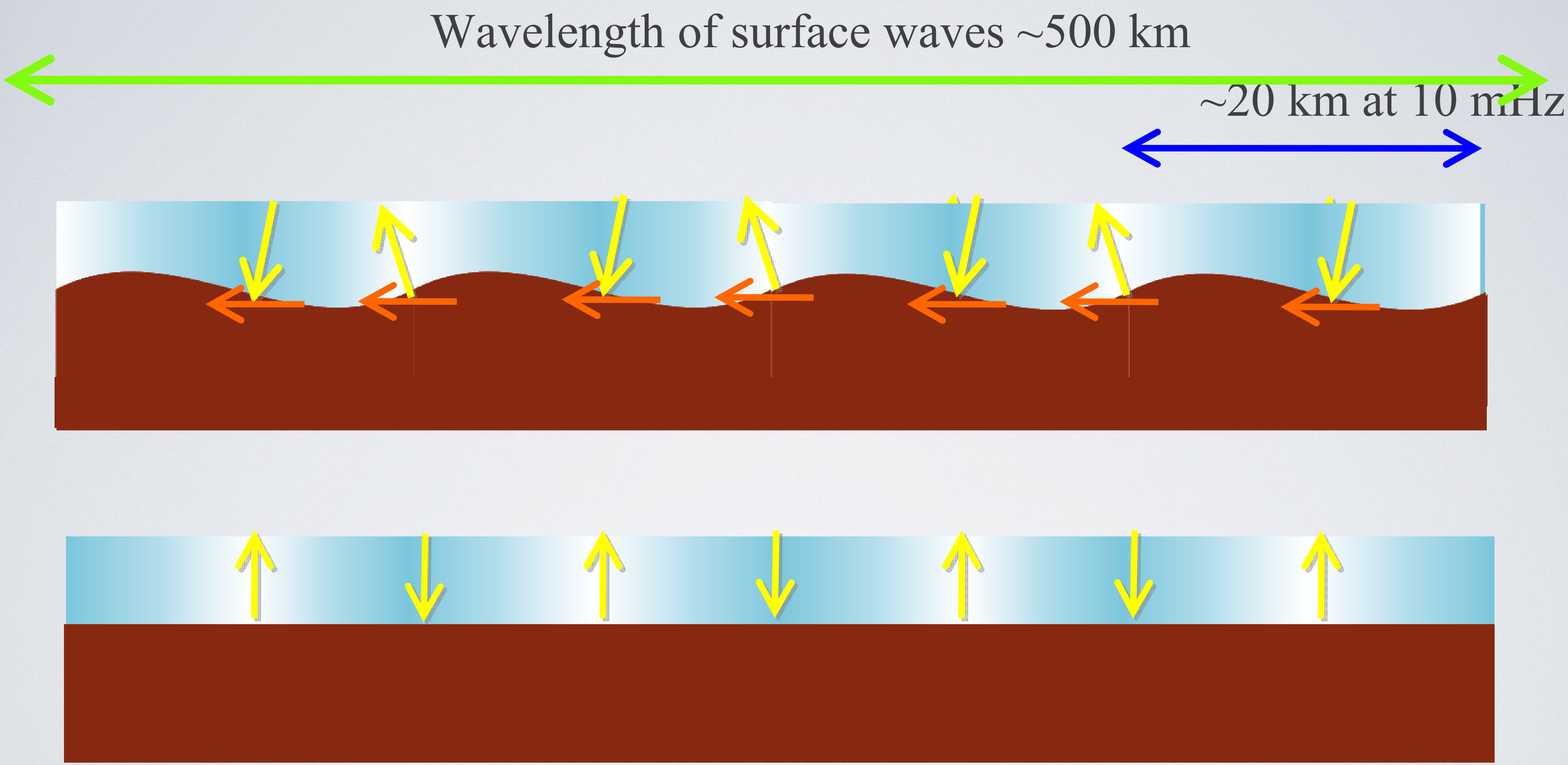

This mechanism can explain observed amplitudes

Fukao et al,

Slant stack analysis: Data set

- Hi-net horizontal accelerometers
  - 679 stations, 2004/6-2004/12
- Data selections
  - Exclusion of data contaminated by large earthquakes (Harvard CMT catalogue)
  - Exclusion of noisy data and local transients

Plots against slowness vector

at 10 mHz

Every two months

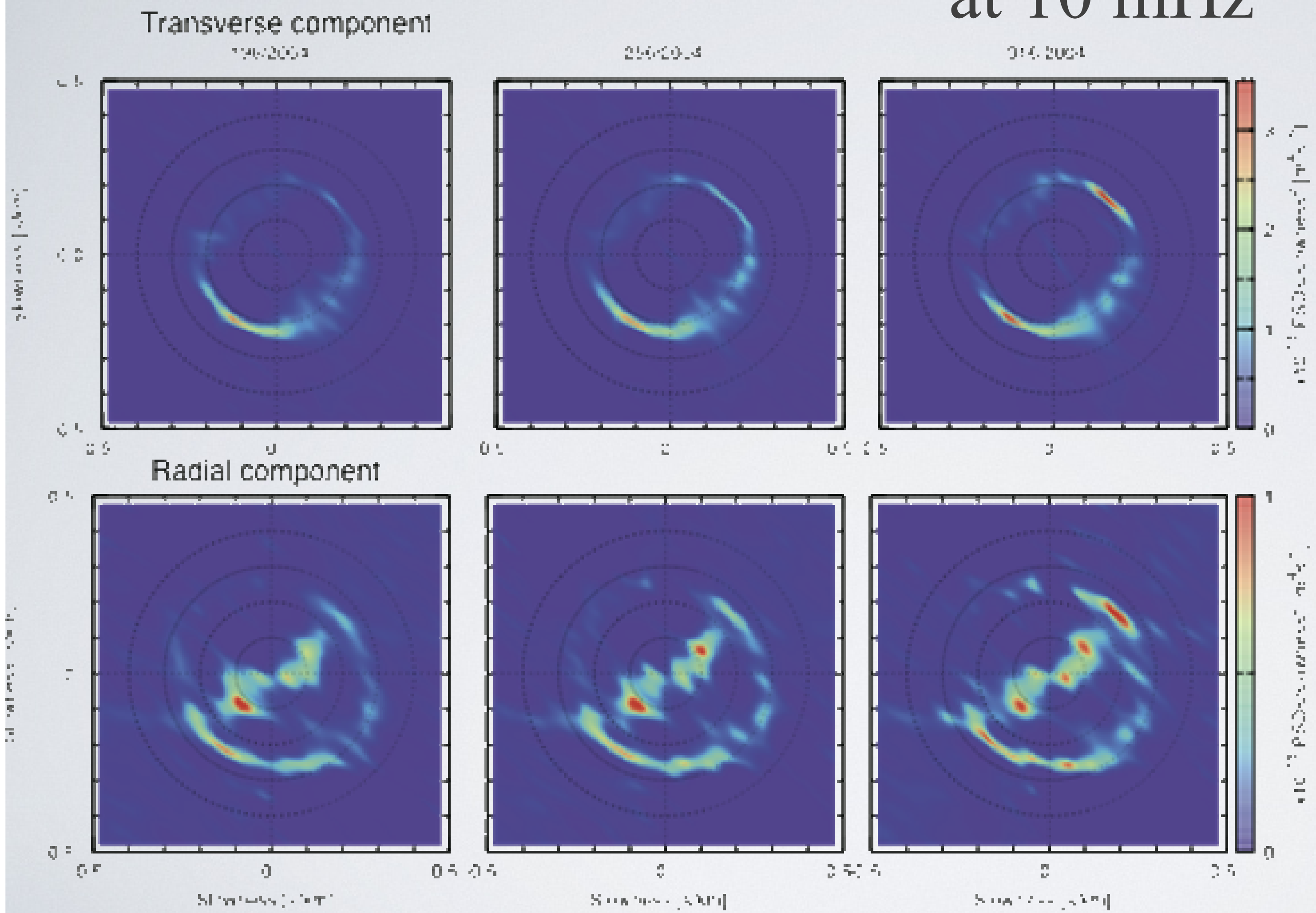

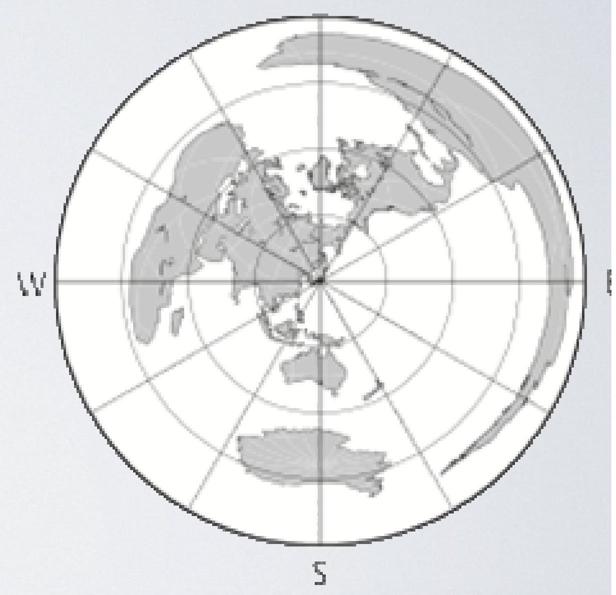

Nishida et al., 2008

Love-wave amplitudes are **3** time lager than Rayleigh-wave ones!!

Why background Love waves?

- Pressure sources cannot excite Love waves for a spherical symmetric Earth
- Features of background Love waves is a key for understanding their excitation mechanism
- Data analysis:
  - Slant stack analysis [Nishida et al., 2008]
  - Auto-correlation analysis [Kurrle and Widmer, 2008]

Power spectra

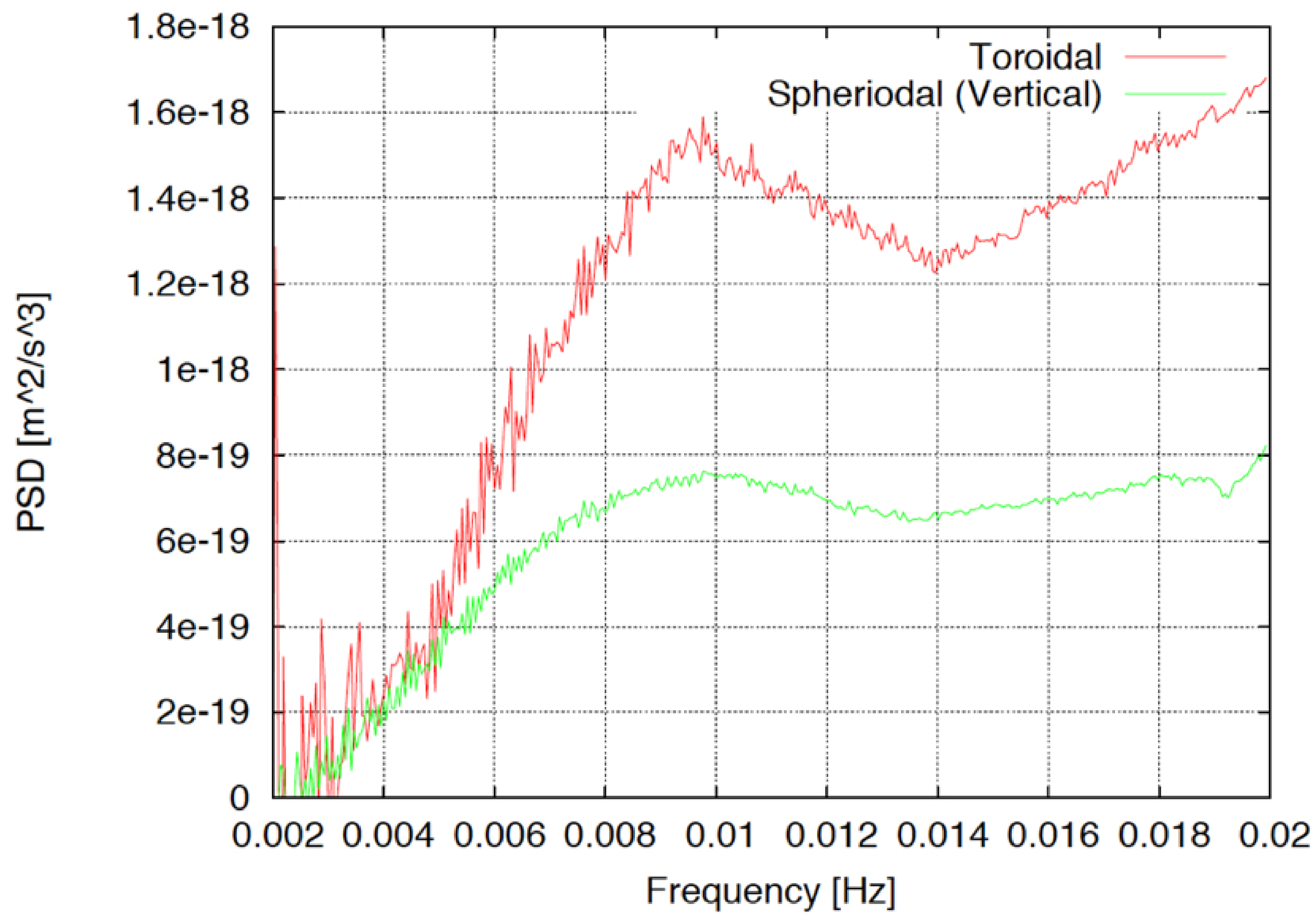

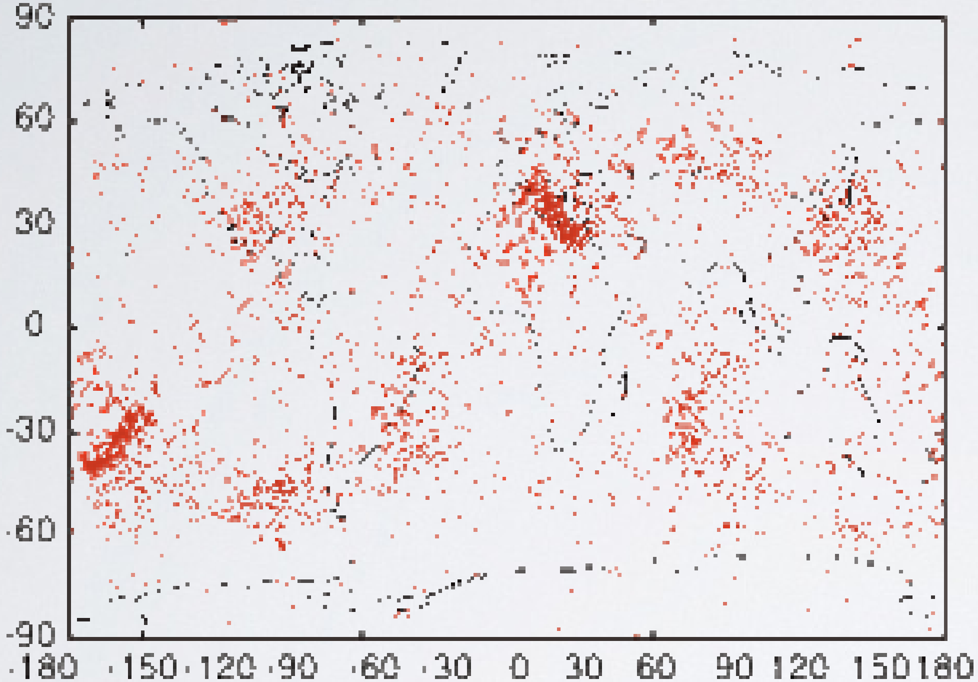
90
60
30
0
-30
-60
-90
-180
-150
-120
-90
-60
-30
0
30
60
90
120
150
180